Journal of Medicinal Chemistry

Article

pubs.acs.org/jmc

Human Toll-Like Receptor 8-Selective Agonistic Activities in 1-Alkyl-1*H*-benzimidazol-2-amines

Mallesh Beesu,[†] Subbalakshmi S. Malladi,[†] Lauren M. Fox,[†] Cassandra D. Jones,[†] Anshuman Dixit,[‡] and Sunil A. David*,[†]

[†]Department of Medicinal Chemistry, University of Kansas, Lawrence, Kansas 66047, United States

[‡]Department of Translational Research and Technology Development, Institute of Life Sciences, Nalco Square, Bhubaneswar 751023, India

Supporting Information

ABSTRACT: Toll-like receptor (TLR)-8 agonists strongly induce the production of T helper 1-polarizing cytokines and may therefore serve as promising candidate vaccine adjuvants, especially for the very young and the elderly. Earlier structure-based ligand design led to the identification of 3-pentyl-quinoline-2-amine as a novel, human TLR8-specific agonist. Comprehensive structure−activity relationships in ring-contracted 1-alkyl-1*H*-benzimidazol-2-amines were undertaken, and the best-in-class compound, 4-methyl-1-pentyl-1*H*-benzo[*d*]imidazol-2-amine, was found to be a pure TLR8 agonist, evoking strong proinflammatory cytokine and Type II interferon responses in human PBMCs, with no attendant CD69 upregulation in natural lymphocytic subsets. The 1-alkyl-1*H*-benzimidazol-2-amines represent a novel, alternate chemotype with pure TLR8-agonistic activities and will likely prove useful not only in understanding TLR8 signaling but also perhaps as a candidate vaccine adjuvant.

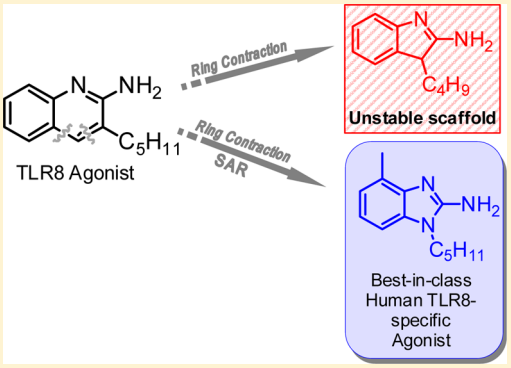

INTRODUCTION

Although the role of vaccines in mitigating morbidity and mortality attributable to infectious diseases in modern times is indisputable,[1,2] we are witnessing a reemergence of infectious diseases previously declared eliminated in the United States. The Centers for Disease Control, for instance, reports 154 cases of measles during the first four months of 2014, a number poised to surpass the 2011 outbreak (the largest since 1996)—even as the recent World Health Organization (WHO) report[3] on antimicrobial resistance warns that "a post-antibiotic era, in which common infections and minor injuries can kill—far from being an apocalyptic fantasy, is instead a very real possibility for the 21st Century". We can neither afford to rest on the numerous and extraordinary successes in preventive medicine nor cease to remind ourselves of the challenges that are yet to be overcome in developing effective vaccines against "old foes" such as the human immunodeficiency virus (HIV), tuberculosis, or malaria.

The main thrust of immunization programs worldwide is generally on vaccinating infants and young children, and it is pertinent to note in this context the WHO's efforts[4] toward developing policy recommendations regarding immunization beyond childhood and into old age. The elderly represent a particularly vulnerable subset of the population. The proportion of the world's population aged 60 and older is estimated to increase from 10% at present to about 21% by 2050.[5] In the United States, the annual mortality of vaccine-preventable diseases in older adults is estimated to be about 50,000−70,000 (compared to 1000−3000 children),[5,6] emphasizing the need for effective immunization strategies adapted specifically for the epidemiological characteristics of the spectrum of infectious diseases in the elderly. Efforts toward optimizing vaccines for the elderly have included increasing antigen dosage[7] as well as the development of better vaccine adjuvants.[8,9]

Vaccine adjuvants are immune potentiators which initiate early innate immune responses leading to the induction of robust and long-lasting adaptive immune responses.[10−14] Until the relatively recent approval of 3-*O*-desacyl-4′-monophosphoryl lipid A (MPL) by the FDA,[15−17] aluminum salts (primarily phosphate and hydroxide), discovered by Glenny and co-workers in 1926,[18] have been the only adjuvants in clinical use. Aluminum salts are weak adjuvants for antibody induction, promoting a T_H2-skewed, rather than a T_H1 response,[19,20] and are virtually ineffective at inducing cytotoxic T lymphocyte or mucosal IgA antibody responses.

Innate immune signals activated by candidate vaccine adjuvants include those originating from Toll-like receptors (TLRs)[21−23] as well as RIG-I-like receptors[24] and NOD-like receptors (NLRs).[25,26] There are 10 functional TLRs encoded in the human genome, which are trans-membrane proteins with an extracellular domain having leucine-rich repeats (LRR) and a cytosolic domain called the Toll/IL-1 receptor (TIR) domain.[22] The ligands for these receptors are highly conserved molecules such as lipopolysaccharides (LPS) (recognized by TLR4, also the

Received: May 6, 2014
Published: August 7, 2014

   dx.doi.org/10.1021/jm500701q | *J. Med. Chem.* 2014, 57, 7325−7341

Scheme 1[a]

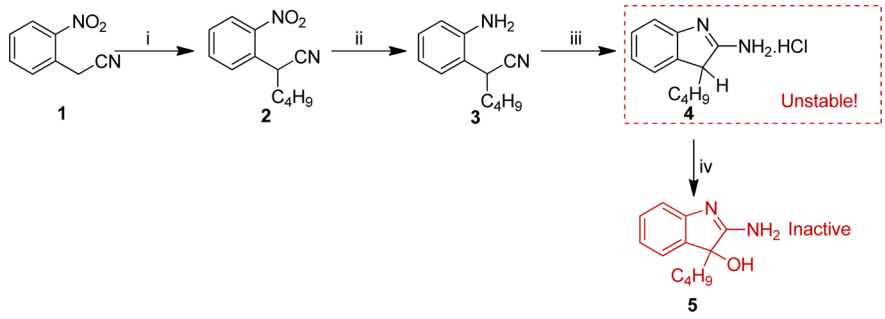

[a]Reagents and conditions: (i) C_4H_9I, K_2CO_3, DMSO, 3 h; (ii) H_2, Pt/C, 30 psi, EtOAc, 3 h; (iii) HCl, dioxane, MW400W, 100 °C, 20 min; (iv) Et_3N, MeOH, 3 h.

target of MPL), lipopeptides (TLR2 in combination with TLR1 or TLR6), flagellin (TLR5), single stranded RNA (TLR7 and TLR8), double stranded RNA (TLR3), CpG motif-containing DNA (recognized by TLR9), and profilin present on uropathogenic bacteria (TLR11).[22] TLR1, -2, -4, -5, and -6 recognize extracellular stimuli, while TLR3, -7, -8, and -9 function within the endolysosomal compartment. The activation of TLRs by their cognate ligands leads to production of inflammatory cytokines and up-regulation of major histocompatibility complex (MHC) molecules and costimulatory signals in antigen-presenting cells as well as activating natural killer (NK) cells (innate immune response), which leads to the priming and amplification of T-, and B-cell effector functions (adaptive immune responses).[21,22,27]

In the course of the last five years we have systematically explored[28−45] a variety of TLR agonists with a view to identifying safe and potent vaccine adjuvants. The chemotypes that we have explored thus far include agonists of TLR2,[30,37,40,41] TLR7,[29,34,35,38,42,43,46] TLR8,[28,31,32,36,46] and nucleotide oligomerization domain 1 (NOD1)[39] as well as C−C chemokine receptor type 1 (CCR1).[33]

Our interest in small molecule agonists of TLR8 as vaccine adjuvants was, in part, kindled by the necessity of having to first identify chemotypes with pure TLR8 activity, given that the known agonists of TLR8 such as the imidazoquinolines,[43,46,47] thiazoloquinolines,[31,48−51] and the 2-aminobenzazepines[52] were found to exhibit mixed TLR7/TLR8-agonism. Our discovery of the 2,3-diamino-furo[2,3-*c*]pyridines[36] and 4-amino-furo-[2,3-*c*]quinolines,[32] leading to structure-based design of the 3-alkyl-quinoline-2-amines[28] as pure TLR8 agonists with no detectable TLR7 activity, was also motivated by observations that the strongly Th1-biasing TLR8 agonists could be useful as candidate vaccine adjuvants for the newborn.[53,54] Maternal immunoglobulins acquired by passive transplacental passage confer protection to the neonate for the first few weeks of life;[55] thereafter, the newborn is susceptible to a wide range of pathogens until early infancy. The very young do not mount adequate adaptive immune responses and, consequently, even highly effective vaccines that confer excellent protection in adults may fail to elicit strong immune responses in them.[56,57] The neonatal immunophenotype is characterized by decreased production of both type I and type II interferons, as well as Th1-biasing cytokines such as TNF-α, IL-12, IL-18, IL-23, the preferential induction of memory B lymphocytes rather than immunoglobulin-secreting plasma cells, as well as a pronounced T-helper type 2 (Th2) skewing of T-cell responses.[58,59] TLR8 agonists induce the production of IL-12, IL-18 and IFN-γ[28,31,32] and may therefore be of value in developing vaccines for the neonate.

Our initial interest in TLR8 agonists as candidate adjuvants has been sustained also by observations of impaired TLR signaling[60−62] contributing to immune senescence[63−65] in aging. In particular, substantial decreases in TNF-α, IL-6, and/or IL-12p40 production have been documented in myeloid dendritic cells isolated from older individuals in response to TLR8 engagement,[60−62] reflecting parallels in immune ontogeny of TLR-driven cytokine responses between the very young and the aged—perhaps an echo of Shakespeare's characterization of the "Seventh Age".

A high-resolution (1.8 Å) structure of human TLR8 co-crystallized with a pure TLR8-agonistic lead compound (C2-butyl-furo[2,3-*c*]quinoline) suggested that the furan ring was dispensable and led to the identification of 3-pentyl-quinoline-2-amine as a novel, structurally simple, and highly potent human TLR8-specific agonist.[28] We now report detailed structure−activity relationships in the ring-contracted 1-alkyl-1*H*-benzimidazol-2-amines. The best-in-class compound of this novel chemotype, 4-methyl-1-pentyl-1*H*-benzo[*d*]imidazol-2-amine, was found to retain a pure TLR8 agonistic activity profile.

RESULTS AND DISCUSSION

With 3-pentyl-quinoline-2-amine as our point of departure, we initially targeted the ring-contracted 2-amino-3-alkylindole analogue **4**, accessed via sequential C-alkylation of commercially available 2-nitrophenylacetonitrile, reduction of the 2-nitro group, and Brønsted acid-promoted, microwave-assisted intramolecular cyclization (Scheme 1). The hydrochloride salt of **4** was isolated and found to be inactive; its free-base, however, was exceedingly unstable, leading to the rapid formation of the overoxidized 3-ol derivative **5**, presumably via autoxidation[66] (Scheme 1), which was also inactive in primary screens.

We therefore focused our attention on stable analogues possessing structural scaffolds similar to the 2-aminoindole **4** and began our investigations with 1-alkyl-2-aminobenzimidazole analogues (Scheme 2). The 2-aminobenzimidazole scaffold was conveniently accessed via the reaction of *o*-phenylenediamine with cyanogen bromide (CNBr). The *N*1 position could be selectively derivatized (Scheme 2), furnishing analogues that we were particularly interested in. In a focused SAR assessment of these analogues, a clear dependence of substituent chain length at *N*1 was noted, consistent with our previous observations on other chemotypes, with the optimal analogue being **8b** (*N*1-pentyl; EC_{50} = 3.23 μM; Figure 1). We specifically desired to examine analogues with benzyl (**8d**) and 3-aminomethylbenzyl (**8f**) substituents at *N*1,

dx.doi.org/10.1021/jm500701q | J. Med. Chem. 2014, 57, 7325−7341

Scheme 2[a]

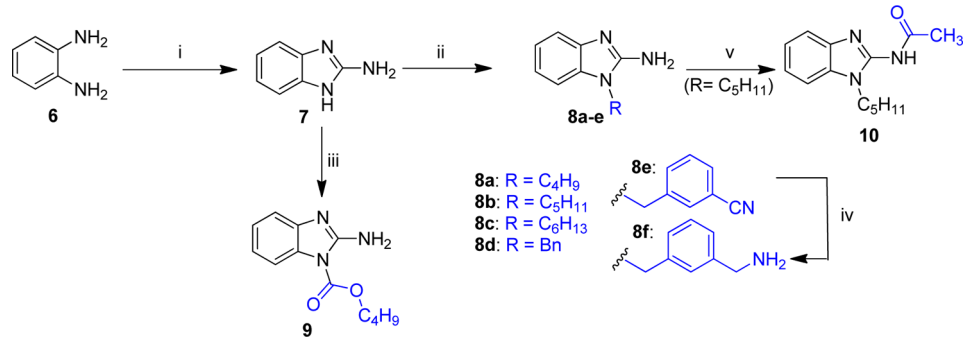

[a]Reagents and conditions: (i) CNBr, MeOH:H_2O (1:1), 60 °C, 3 h; (ii) RI, KOH, acetone, 60 °C, 3 h; (iii) C_4H_9OCOCl, THF, 25 °C, 3 h; (iv) $LiAlH_4$, THF, 75 °C, 5 h; (v) CH_3COCl, pyridine, 25 °C, 3 h.

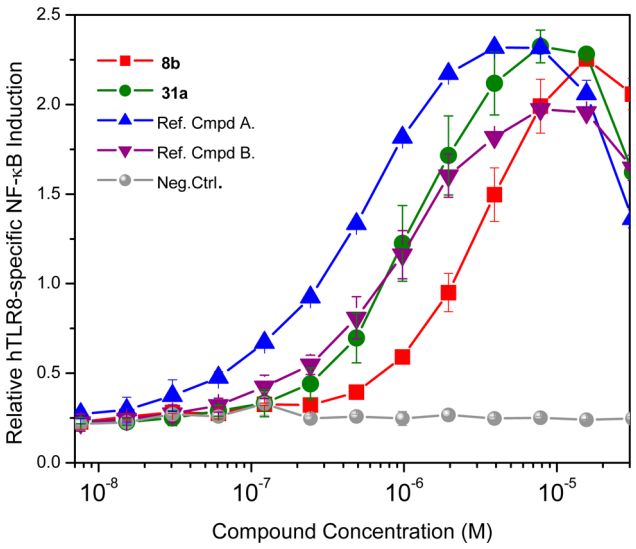

Figure 1. Dose−response profiles by select 1-alkyl-1*H*-benzimidazol-2-amines in reporter gene cells expressing human TLR8. Error bars represent standard deviations obtained on quadruplicates. Reference compounds **A** and **B** (pure TLR8 agonists) are 3-pentyl-quinoline-2-amine[28] and C2-butyl-furo[2,3-*c*]quinoline,[32] respectively.

for these substituents on the imidazoquinoline scaffold had yielded high-potency pure TLR7 and mixed TLR8/7 agonists, respectively.[43] Somewhat to our surprise, we found that neither **8d** nor **8f** were active; substitution of the *N*1-pentyl group with butoxycarbonyl group (**9**) or acylation of the *N*2 amine (**10**) also completely abrogated activity, suggestive of stringent structural requirements for activity and demonstrating that both the free amine at C2 and the *N*1 pentyl substituent are important for TLR8- agonistic activity.

We addressed modifications on the benzimidazole core, mindful of our previous observations of benzologues of imidazo[4,5-*c*]pyridines showing specific TLR7 activity.[29] We therefore synthesized all possible regioisomeric benzologues of **8b** (Scheme 3). The naphtho-[2,3-*d*]imidazole analogue **13** was accessed readily via cyclization of the naphthalene-2,3-diamine with CNBr. The symmetry-related regioisomers **18** and **23** could, in principle, have been obtained from the rather expensive 1,2-diaminonaphthalene, followed by resolution of the regioisomers. But given the near-identical R_f values (and retention times in analytical HPLC) of these two regioisomers, we were fortunate (in hindsight) to have opted for an alternative route. We had originally envisaged a sequence of chlorination of 1-nitronaphthalen-2-ol and 2-nitronaphthalen-1-ol precursors, nucleophilic substitution with pentylamine, and subsequent formation of the aminoimidazole ring; however, conversion of the nitronaphthols to corresponding chloronitronaphols proved unexpectedly problematic. This was alleviated by conversion to the nitromethoxynaphthols **15** and **20**, which underwent facile nucleophilic substitution reactions with pentylamine, affording the desired regioisomers **18** and **23** in good yields (Scheme 3). Of the three different regioisomers, only **23** (EC_{50} = 3.16 μM) showed near-identical activity to that of **8b** (Table 1). These observations, taken together, also suggested that substitutions could be tolerated at C4 and C5, but not at C6 and C7, which were borne out as described below.

We next targeted all possible regioisomers of imidazopyridines (**27a−d**) for possible TLR7/8 activity, given that these analogues are congeneric to the imidazo[4,5-*c*] pyridines[29] (Scheme 4). These analogues were synthesized via S_NAr reactions of corresponding *o*-halonitropyridines with pentylamine, reduction of the nitro group, and final cyclization with CNBr (Scheme 4). None of these analogues were active, and it remained for us to explore substitutions on the benzimidazole core. In our final salvo, therefore, we systematically introduced methyl substituents at C4−C7 positions (**31a−d**, Scheme 5) to ascertain steric effects of the benzimidazole ring and their consequences on biological activity. Only **31a**, with a C4-methyl group showed significantly more potent activity (EC_{50} = 1.13 μM), relative to the parent compound **8b**; the potency was comparable to that of C2-butyl-furo[2,3-*c*]quinoline[32] and marginally less than that of 3-pentyl-quinoline-2-amine[28] (Figure 1). We also examined different electron-donating and -withdrawing substituents at C4 position. The methoxy analogue **31e** (EC_{50} = 3.74 μM) showed comparable activity to that of **8b** but was less active than **31a** (Table 1). Electron-withdrawing substitutions (**31f−i**) resulted in inactive compounds. Homologation of the methyl group at C4 to the ethyl-substituted analogue **31j** (accomplished via Suzuki coupling of 3-bromo-2-nitro-*N*-pentylaniline with ethylboronic acid and subsequent elaboration; Scheme 5) resulted in a slight reduction in TLR8-agonistic potency compared to **31a**, alerting us to the possibility that longer (or bulkier) substituents would not be favorable and, indeed, phenyl (**31l**), benzyl (**31m**), or benzyloxy (**35**) substituents at C4 abrogated activity. The electron-deficient 4-nitro analogue **39** (Scheme 7) was inactive, and analogues with electron-donating groups at C4 (**31k**, **36**, **40**; Schemes 5−7) displayed attenuated potency relative to the 4-methyl compound **31a** (Table 1).

We employed induced-fit docking methods[32] to compare the binding modes of the 2-aminobenzimidazole analogues with known TLR8 ligands, utilizing high-resolution crystal structures of human TLR8.[28,67] The TLR8-active analogues such as **8b** and

dx.doi.org/10.1021/jm500701q | J. Med. Chem. 2014, 57, 7325−7341

Scheme 3[a]

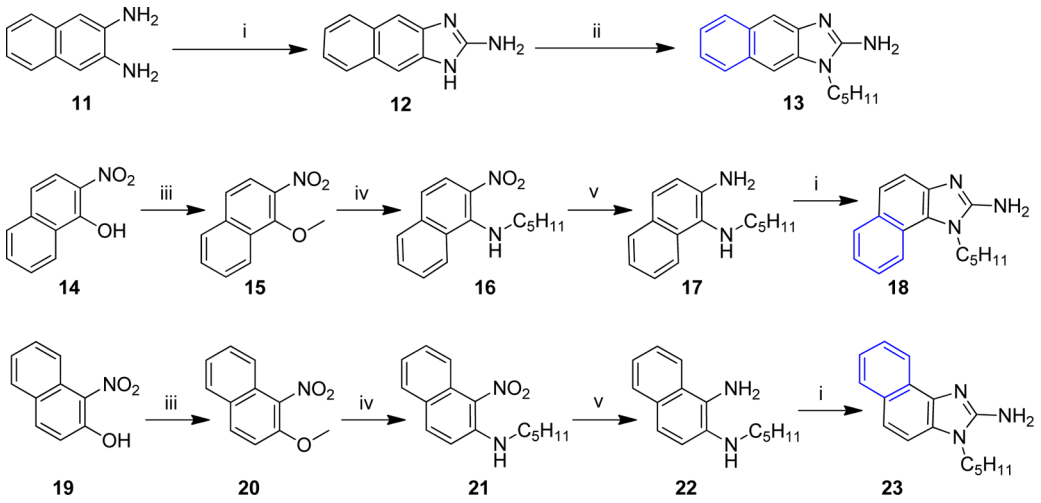

[a]Reagents and conditions: (i) CNBr, MeOH:H_2O (1:1), 60 °C, 3 h; (ii) $C_5H_{11}I$, KOH, acetone, 60 °C, 3 h; (iii) MeI, KOH, acetone, reflux, 12 h; (iv) $C_5H_{11}NH_2$, DMF, 60 °C, 12 h; (v) H_2, Pt/C, 30 psi, EtOAc, 3 h.

31a occupy the binding pocket formed by both of the TLR8 protomers with the expected binding geometry involving strong bidentate ionic H bonds between Asp543 of TLR8 and both the C2 amine as well as the *N*3 atom of the benzimidazole compounds (Figure 2). Stabilization derived from an H bond between Thr574 (protomer B) and the C2-NH_2 as well as hydrophobic interactions of the *N*1-alkyl group with the hydrophobic pocket lined by Phe346/Ile403/Gly376 within protomer A were also observed as reported earlier.[28] Favorable $\pi-\pi$ interactions of the phenyl ring of the bezimidazoles and Phe405 were observed. We were, in particular, interested in understanding why only the C4-methyl analogue **31a**, and not congeners bearing methyl groups at C5, C6, or C7 (**31b–d**, respectively), showed enhanced potency relative to **8b**. An examination of **31a** bound to TLR8 showed favorable van der Waals interactions (3.7 Å) between the C4-methyl and the side chain of Val520 (Figure 2A), which become unfavorable (5.2 Å) in the C5-methyl analogue **31b** and lost entirely in **31c** and **31d** (not shown). The occupancy of the benzologues **13**, **18** and **23** in the binding pocket is compromised by unfavorable sterics, exemplified in the case of **13**, forcing the binding of the analogue in an inverted fashion with the consequent loss of the critical H-bond interactions between the C2 amine and Asp543 (Figure 2B). As detailed above, the docking studies allowed a rationalization of binding activities in terms of steric properties of the analogues but proved less useful in understanding electronic effects. For instance, favorable binding geometries and energies were also observed for the inactive pyridyl analogues **27a–d**, pointing to limitations inherent in force field computations.[68]

All analogues were counter-screened in agonism screens using reporter cell lines specific for human TLR2, TLR3, TLR4, TLR5, TLR7, TLR9, NOD1, and NOD2 (Figures S1 and S2). No off-target effects were detected, confirming the specificity of the active analogues for human TLR8. Certain benzimidazoles such as Noditinib-1[69] (1-[(4-methylphenyl)sulfonyl]-1*H*-benzimidazol-2-amine) have been shown to inhibit NOD-1 signaling, and it was therefore of interest to also characterize possible antagonistic activities. Weak antagonistic activities (IC_{50}: >10 μM) toward NOD-1 and NOD-2 were observed for **10**, **13**, **18**, **31l**, **31m**, and **35** (Figure S3); these results suggested that bulky substituents at C4 may yield NOD-1/NOD-2 antagonists but were not a priority for us in the context of discovering novel vaccine adjuvants.

The best-in-class of this novel TLR8-agonistic chemotype, **31a** was taken forward and characterized further in cytokine/chemokine induction profiles in a panel of secondary screens employing human peripheral blood mononuclear cells, as well as whole human blood. Consistent with its specificity for TLR8, we observed induction of proinflammatory cytokines, as well as IL-12p40 and IFN-γ (Figure 3), and a complete absence of CD69 upregulation in NK lymphocytes (Figure 4). We had previously shown that CD69 upregulation in NK cells is ascribable purely to TLR7 activity,[28,32] and these results confirm absolute specificity of the lead 2-aminobenzimidazole compounds for human TLR8. CD69 is a type II C-lectin membrane receptor with immunoregulatory functions.[70,71] The absence of CD69 (in CD69 knockout mice) is correlated with increased generation of Th1 lymphocytes and enhanced production of Th1-biasing cytokines,[72,73] consistent with our observation of induction of high levels of IL-12 and IFN-γ in human PBMCs (Figure 4).

In summary, the 1-alkyl-1*H*-benzimidazol-2-amines represent a novel chemotype with human TLR8-specific agonistic activities, which will likely prove useful not only as tools to dissect TLR7 vis-à-vis TLR8 signaling but also as candidate vaccine adjuvants with strong Th1 bias.

EXPERIMENTAL SECTION

Chemistry. All of the solvents and reagents used were obtained commercially and used as such unless noted otherwise. Moisture- or air-sensitive reactions were conducted under nitrogen atmosphere in oven-dried (120 °C) glass apparatus. Solvents were removed under reduced pressure using standard rotary evaporators. Flash column chromatography was carried out using RediSep Rf "Gold" high-performance silica columns on CombiFlash R_f instruments unless otherwise mentioned, while thin-layer chromatography was carried out on silica gel CCM precoated aluminum sheets. Purity for all final compounds was confirmed to be >98% by LC-MS using a Zorbax Eclipse Plus 4.6 × 150 mm, 5 μm analytical reverse phase C_{18} column with H_2O-CH_3CN and H_2O-MeOH gradients and an Agilent 6520 ESI-QTOF Accurate Mass spectrometer (mass accuracy of 5 ppm) operating in the positive ion acquisition mode.

2-(2-Nitrophenyl)hexanenitrile (**2**). To a solution of 2-nitrophenylacetonitrile (162 mg, 1 mmol) in anhydrous DMSO (5 mL) was added K_2CO_3 (152 mg, 1.1 mmol), and the reaction mixture was stirred

dx.doi.org/10.1021/jm500701q | J. Med. Chem. 2014, 57, 7325–7341

Table 1. EC_{50} Values of Compounds in Human TLR 8-Specific Reporter Gene Assays

Compound Number	Structure	hTLR8 Agonistic Activity (μM)
4	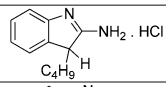	Unstable
5	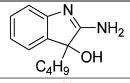	Inactive
8a	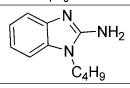	7.30
8b	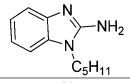	3.23
8c	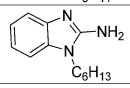	3.96
8d	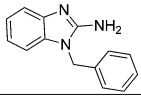	Inactive
8f	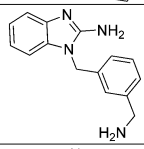	Inactive
9	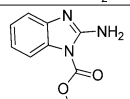	Inactive
10	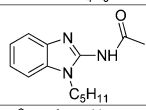	Inactive
13	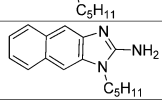	Inactive
18	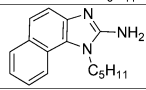	Inactive
23	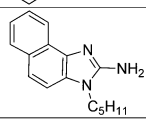	3.16
27a	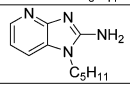	Inactive
27b	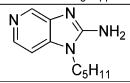	Inactive
27c	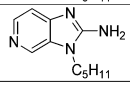	Inactive
27d	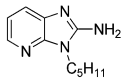	Inactive
31a	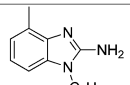	1.13
31b	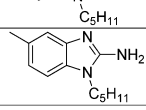	4.57

Compound Number	Structure	hTLR8 Agonistic Activity (μM)
31c	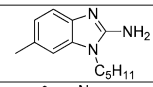	7.21
31d	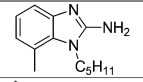	6.61
31e	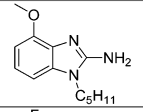	3.74
31f	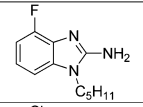	Inactive
31g	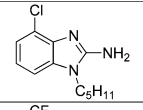	Inactive
31h	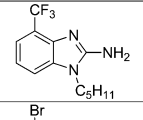	Inactive
31i	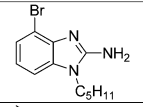	Inactive
31j	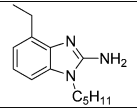	1.65
31k	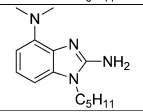	7.12
3ll	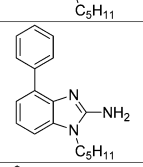	Inactive
31m	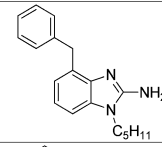	Inactive
35	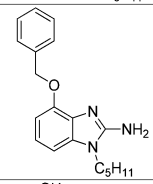	Inactive
36	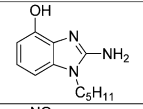	5.01
39	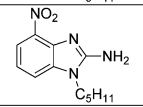	Inactive
40	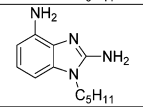	6.60

for 10 min under nitrogen atmosphere. Butyl iodide (125 μL, 1.1 mmol) was added to the reaction mixture, and the stirring was continued for 3 h. Water was added to the reaction mixture, and it was extracted with EtOAc (3 × 20 mL). The combined organic layer was dried over Na_2SO_4 and concentrated under reduced pressure, and the crude material was purified by silica gel column chromatography (10% EtOAc/hexanes) to afford

dx.doi.org/10.1021/jm500701q | J. Med. Chem. 2014, 57, 7325−7341

Scheme 4[a]

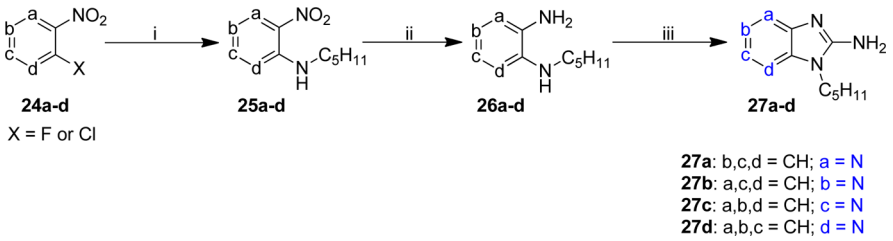

[a]Reagents and conditions: (i) $C_5H_{11}NH_2$, DIPEA, DMSO, 60 °C, 6 h; (ii) H_2, Pt/C, 30 psi, EtOAc, 3 h; (iii) CNBr, MeOH:H_2O (1:1), 60 °C, 3 h.

Scheme 5[a]

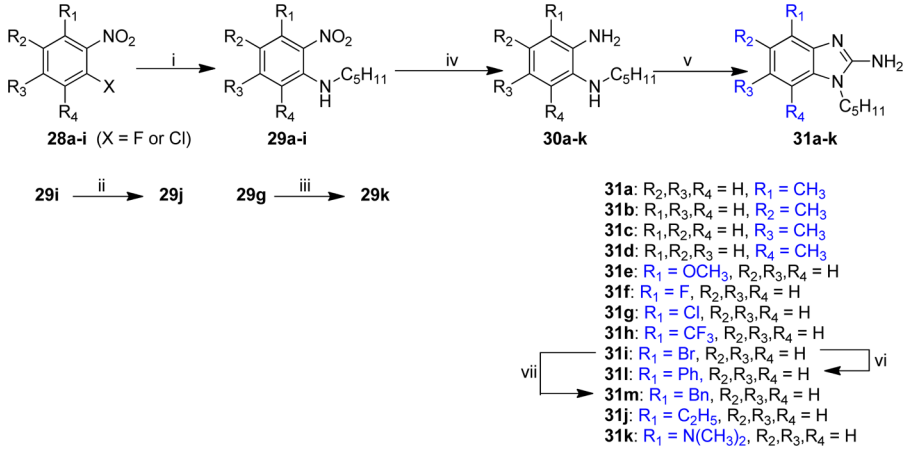

[a]Reagents and conditions: (i) $C_5H_{11}NH_2$, DIPEA, DMSO, 60 °C, 12 h; (ii) C_2H_5-B(OH)$_2$, K_2CO_3, Pd(dppf)Cl_2,1,4-dioxane, 90 °C, 12 h; (iii) $HN(CH_3)_2$, DMF, 90 °C, 12 h; (iv) H_2, Pt/C, 30 psi, EtOAc, 3 h; (v) CNBr, MeOH:H_2O (1:1), 60 °C, 3 h; (vi) C_6H_5-B(OH)$_2$, K_2CO_3, Pd(dppf)Cl_2, 1,4-dioxane, 90 °C, 12 h; (vii) benzylzinc bromide, Pd(dppf)Cl_2, THF, 70 °C, 12 h.

Scheme 6[a]

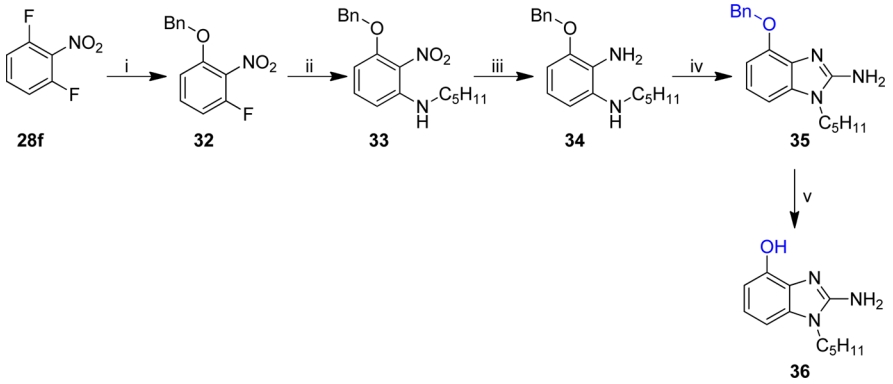

[a]Reagents and conditions: (i) $C_6H_5CH_2OH$, K_2CO_3, DMF, 60 °C, 12 h; (ii) $C_5H_{11}NH_2$, DIPEA, DMSO, 60 °C, 12 h; (iii) H_2, Pt/C, 30 psi, EtOAc, 3 h; (iv) CNBr, MeOH:H_2O (1:1), 60 °C, 3 h; (v) H_2, Pd/C, 30 psi, MeOH, 3 h.

Scheme 7[a]

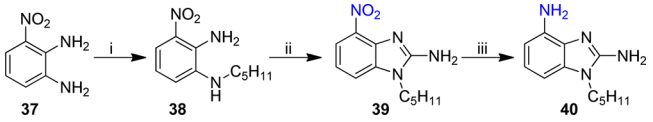

[a]Reagents and conditions: (i) $C_5H_{11}I$, K_2CO_3, DMF, 50 °C, 12 h; (ii) CNBr, MeOH:H_2O (1:1), 60 °C, 3 h; (iii) H_2, Pt/C, 30 psi, EtOAc, 3 h.

compound **2** as a pale yellow oil (174 mg, 80%). R_f = 0.50 (10% EtOAc/hexanes). ^{1}H NMR (500 MHz, $CDCl_3$) δ 8.05 (dd, J = 8.2, 1.3 Hz, 1H), 7.79 (dd, J = 7.9, 1.4 Hz, 1H), 7.70 (td, J = 7.6, 1.3 Hz, 1H), 7.52 (ddd, J = 8.6, 7.5, 1.4 Hz, 1H), 4.70 (dd, J = 9.5, 4.9 Hz, 1H), 2.01−1.84 (m, 2H), 1.59−1.52 (m, 2H), 1.47−1.32 (m, 2H), 0.93 (t, J = 7.3 Hz, 3H). ^{13}C NMR (126 MHz, $CDCl_3$) δ 147.64, 134.26, 131.59, 130.26, 129.39, 125.77, 120.22, 35.47, 33.98, 29.62, 22.08, 13.90. MS (ESI-TOF) for $C_{12}H_{14}N_2O_2$ $[M + H]^+$ calculated 219.1128, found 219.1095.

*2-(2-Aminophenyl)hexanenitrile (**3**).* To a solution of compound **2** (109 mg, 0.5 mmol) in anhydrous EtOAc (10 mL) was added a catalytic amount of Pt/C (39 mg, 1 mol %), and the reaction mixture was subjected to hydrogenation at 30 psi hydrogen pressure for 3 h. The reaction mixture was filtered, and the filtrate concentrated under reduced pressure. The crude material was purified using silica gel column chromatography (10% MeOH/CH_2Cl_2) to obtain **3** as a pale

dx.doi.org/10.1021/jm500701q | J. Med. Chem. 2014, 57, 7325−7341

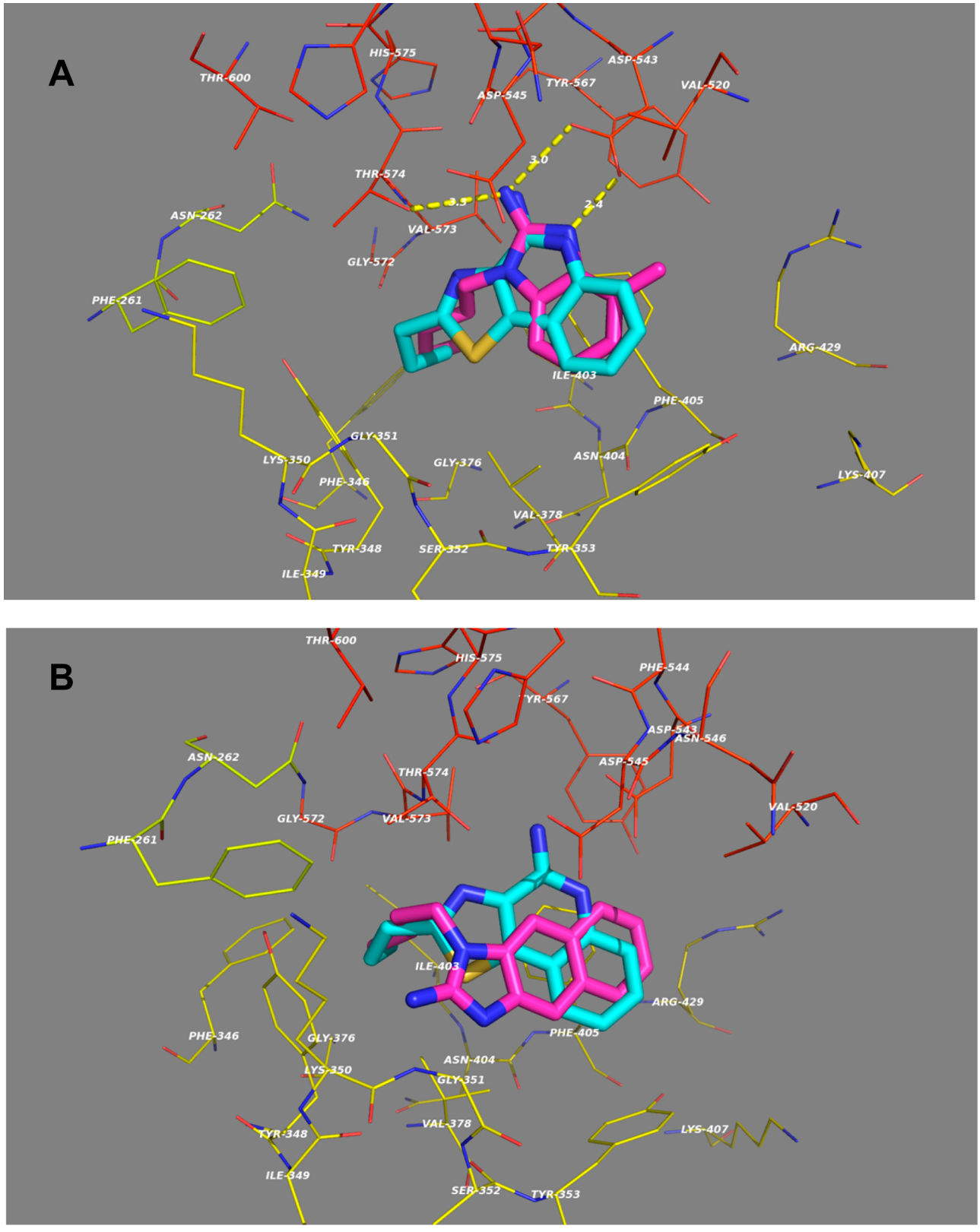

Figure 2. Induced-fit docking of **31a** (Panel A) and **13** (Panel B) in human TLR8 superimposed on the bound conformation of 2-propylthiazolo-[4,5-*c*]quinolin-4-amine (coordinates derived from PDB ID: 3W3K). The protomers of the TLR8 dimer are colored in yellow and red. Strong bidentate ionic H bonds are observed between Asp543 of TLR8 and the C2 amine and the *N*3 atom of **31a** (Panel A). The *N*1-pentyl group shows extensive hydrophobic interactions in the pocket lined by Phe346/Ile403/Gly376 within protomer A, favorable $\pi-\pi$ interactions of the phenyl ring of **31a** and Phe405, and van der Waals interactions between the C4-methyl and the side chain of Val520 (Panel A). The occupancy of the benzologues **13** in the binding pocket is compromised by unfavorable sterics, forcing the binding of the analogue in an inverted fashion with the consequent loss of the critical H-bond interactions between the C2 amine and Asp543 (Panel B).

dx.doi.org/10.1021/jm500701q | *J. Med. Chem.* 2014, 57, 7325−7341

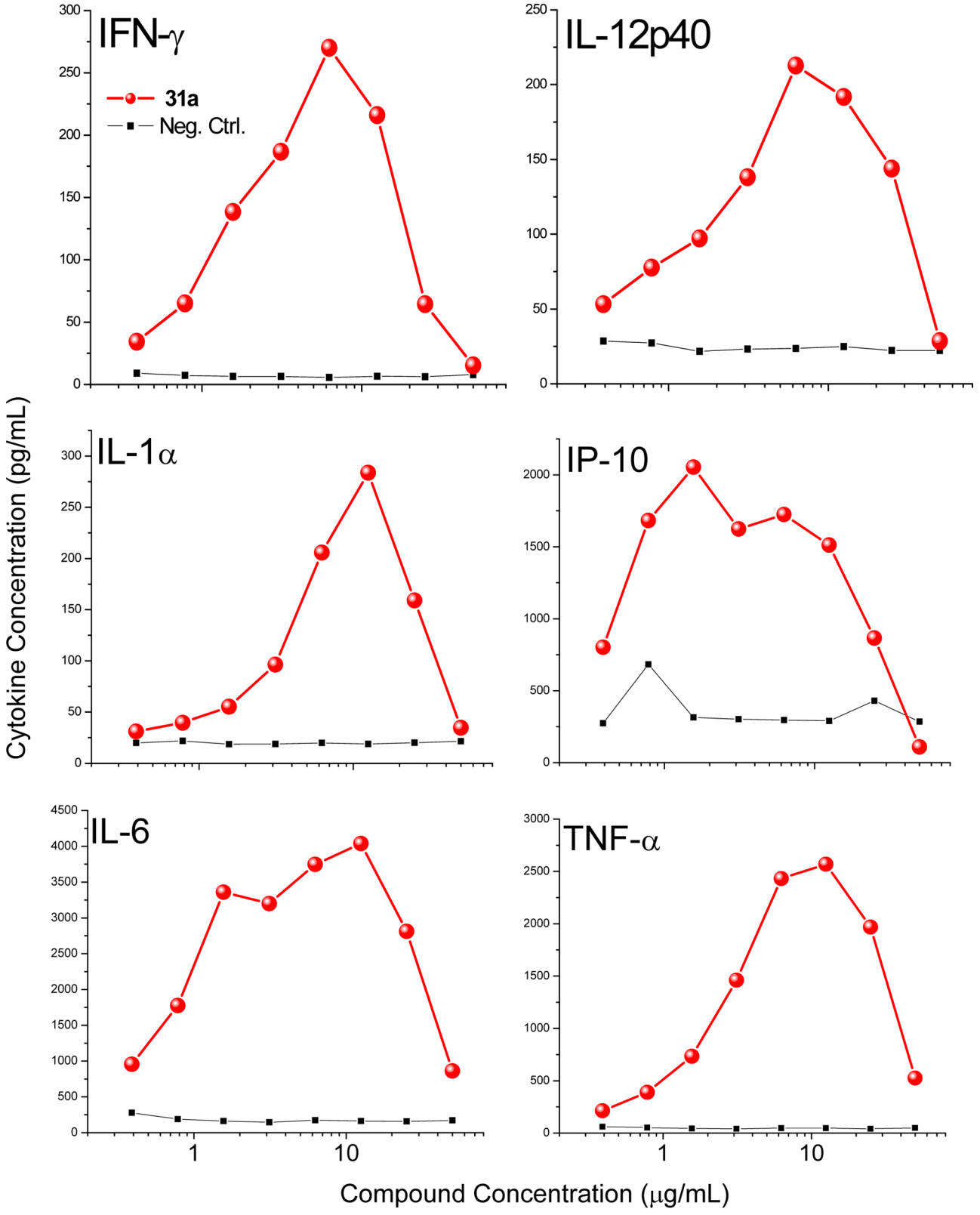

Figure 3. Proinflammatory cytokine induction profiles of **31a** in human blood. Means of duplicate values of a representative experiment is shown.

yellow oil (70 mg, 74%). R_f = 0.40 (10% MeOH/CH_2Cl_2). ^{1}H NMR (500 MHz, $CDCl_3$) δ 7.22 (dd, J = 7.7, 1.4 Hz, 1H), 7.14 (td, J = 7.8, 1.5 Hz, 1H), 6.83 (td, J = 7.5, 1.2 Hz, 1H), 6.73 (dd, J = 8.0, 1.1 Hz, 1H), 3.75 (dd, J = 9.0, 6.0 Hz, 1H), 3.69 (bs, 2H), 2.04−1.94 (m, 1H), 1.91−1.83 (m, 1H), 1.58−1.44 (m, 2H), 1.42−1.33 (m, 2H), 0.92 (t, J = 7.3 Hz, 3H). ^{13}C NMR (126 MHz, $CDCl_3$) δ 143.47, 129.22, 128.70, 120.76, 120.70, 119.85, 117.54, 33.47, 32.24, 29.62, 22.28, 13.96. MS (ESI-TOF) for $C_{12}H_{16}N_2$ $[M + H]^+$ calculated 189.1386, found 189.1359.

*2-Amino-3-butyl-3H-indol-3-ol (**5**).* To a solution of compound **3** (38 mg, 0.2 mmol) in anhydrous dioxane (1 mL) was added 4 N HCl/dioxane (0.1 mL). The reaction mixture was then heated under

dx.doi.org/10.1021/jm500701q | J. Med. Chem. 2014, 57, 7325−7341

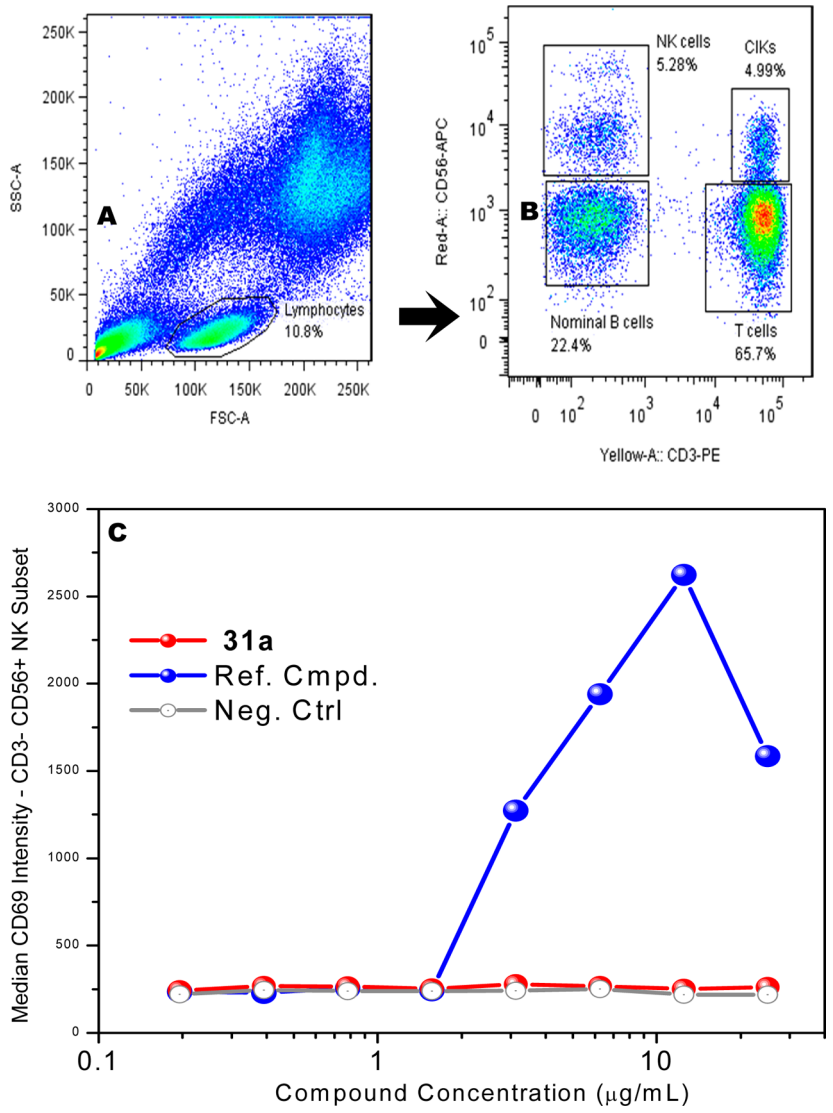

Figure 4. Absence of CD69 upregulation in human natural killer cells by **31a**. (A) PBMCs with primary gates on lymphocytes. (B) Secondary quadrant gates on lymphocytic population showing $CD3^+CD56^-$ (T cells, Quadrant A), $CD3^-CD56^-$ (nominal B cells, Quadrant B), $CD3^+CD56^+$ (cytokine-induced killer cells, Quadrant C), and $CD3^-CD56^+$ (natural killer cells, Quadrant D). (C) CD69 expression in natural killer lymphocytes. Reference compound used was a pure TLR7 agonist (1-benzyl-2-butyl-1*H*-imidazo[4,5-*c*]quinolin-4-amine).[43]

microwave conditions (400 W, 100 °C) in a sealed vial for 20 min. The reaction mixture was cooled to room temperature, and the solvent was removed under reduced pressure to obtain the compound **4**. To a solution of compound **4** in MeOH (1 mL) was added Et_3N (56 μL, 0.4 mmol). The reaction mixture was then stirred for 3 h. The solvent was removed under reduced pressure, and the crude material was purified using silica gel column chromatography (20% $MeOH/CH_2Cl_2$) to obtain the compound **5** as white solid (23 mg, 56%). R_f = 0.30 (20% $MeOH/CH_2Cl_2$). ^1H NMR (500 MHz, DMSO) δ 8.49 (bs, 2H), 7.20 (ddd, J = 11.4, 8.8, 4.2 Hz, 2H), 6.98−6.85 (m, 2H), 6.05 (s, 1H), 1.91 (td, J = 12.6, 4.7 Hz, 1H), 1.80 (td, J = 12.6, 4.7 Hz, 1H), 1.21−1.08 (m, 2H), 0.98−0.80 (m, 2H), 0.75 (t, J = 7.3 Hz, 3H). ^{13}C NMR (126 MHz, DMSO) δ 176.36, 150.46, 135.76, 129.12, 122.59, 121.63, 113.90, 81.06, 37.84, 24.89, 22.18, 13.83. MS (ESI-TOF) for $C_{12}H_{16}N_2O$ $[M + H]^+$ calculated 205.1335, found 205.1358.

*2-Aminobenzimidazole (**7**).* To a solution of compound *o*-phenylenediamine (108 mg, 1 mmol) in 1:1 mixture of MeOH (5 mL) and water (5 mL) was added CNBr (318 mg, 3 mmol). The reaction mixture was stirred for 3 h at 60 °C. The reaction mixture was cooled to room temperature, the MeOH was removed under reduced pressure, and the remaining mixture was basified with 1.0 M aq. NaOH (to pH = 8.0) and extracted with EtOAc (3 × 30 mL). The combined organic layer was dried over Na_2SO_4, concentrated under reduced pressure, and the crude material was purified by silica gel column chromatography (20% $MeOH/CH_2Cl_2$) to obtain the compound **7** as a white solid (109 mg, 82%). R_f = 0.20 (20% $MeOH/CH_2Cl_2$). ^1H NMR (500 MHz, DMSO) δ 10.68 (bs, 1H), 7.12−7.01 (m, 2H), 6.83 (dd, J = 5.7, 3.2 Hz, 2H), 6.11 (s, 2H). ^{13}C NMR (126 MHz, DMSO) δ 155.29, 138.79, 118.95, 111.52. MS (ESI-TOF) for $C_7H_7N_3$ $[M + H]^+$ calculated 134.0713, found 134.0705.

*1-Butyl-1H-benz[d]imidazol-2-amine (**8a**).* To a solution of 2-aminobenzimidazole (**7**) (27 mg, 0.2 mmol) in acetone (1 mL) were added KOH (22 mg, 0.4 mmol) and butyl iodide (23 μL, 0.2 mmol). The reaction mixture was stirred for 3 h at 60 °C. The reaction mixture was cooled to room temperature, and the solvent was removed under reduced pressure. The reaction mixture was diluted with water and extracted with EtOAc (3 × 10 mL). The combined organic layer was dried over Na_2SO_4 and concentrated under reduced pressure, and the crude material was purified by silica gel column chromatography (20% $MeOH/CH_2Cl_2$) to obtain the compound **8a** as a white solid (28 mg, 74%). R_f = 0.45 (20% $MeOH/CH_2Cl_2$). ^1H NMR (500 MHz, $CDCl_3$) δ 7.44 (dd, J = 7.7, 0.8 Hz, 1H), 7.15−7.06 (m, 3H), 4.61 (bs, 2H), 3.92 (t, J = 7.2 Hz, 2H), 1.81−1.74 (m, 2H), 1.45−1.37 (m, 2H), 0.96 (t, J = 7.4 Hz, 3H). ^{13}C NMR (126 MHz, $CDCl_3$) δ 153.15, 141.86,

dx.doi.org/10.1021/jm500701q | J. Med. Chem. 2014, 57, 7325−7341

134.42, 121.59, 119.98, 116.73, 107.95, 42.80, 31.30, 20.41, 13.90. MS (ESI-TOF) for $C_{11}H_{15}N_3$ $[M + H]^+$ calculated 190.1339, found 190.1393.

Compounds **8b**−**8e** were synthesized similarly as compound **8a**.

*1-Pentyl-1H-benzo[d]imidazol-2-amine (**8b**).* 1-Iodopentane was used as reagent. White solid (25 mg, 61%). R_f = 0.50 (20% MeOH/CH_2Cl_2). ^{1}H NMR (500 MHz, DMSO) δ 7.11 (d, J = 1.0 Hz, 1H), 7.09 (d, J = 1.0 Hz, 1H), 6.91 (td, J = 7.4, 1.1 Hz, 1H), 6.85 (td, J = 7.4, 1.1 Hz, 1H), 6.35 (s, 2H), 3.94 (t, J = 7.2 Hz, 2H), 1.66−1.57 (m, 2H), 1.34−1.20 (m, 4H), 0.84 (t, J = 7.0 Hz, 3H). ^{13}C NMR (126 MHz, DMSO) δ 154.81, 142.80, 134.27, 120.09, 117.88, 114.65, 107.44, 41.34, 28.30, 28.18, 21.94, 13.95. MS (ESI-TOF) for $C_{12}H_{17}N_3$ $[M + H]^+$ calculated 204.1495, found 204.1544.

*1-Hexyl-1H-benzo[d]imidazol-2-amine (**8c**).* 1-Iodohexane was used as reagent. White solid (30 mg, 69%). R_f = 0.52 (20% MeOH/CH_2Cl_2). ^{1}H NMR (500 MHz, $CDCl_3$) δ 7.44 (d, J = 7.8 Hz, 1H), 7.16−7.04 (m, 3H), 4.66 (bs, 2H), 3.91 (t, J = 7.3 Hz, 2H), 1.82−1.75 (m, 2H), 1.39−1.25 (m, 6H), 0.88 (t, J = 7.0 Hz, 3H). ^{13}C NMR (126 MHz, $CDCl_3$) δ 153.25, 142.00, 134.43, 121.53, 119.92, 116.72, 107.92, 43.02, 31.59, 29.20, 26.82, 22.64, 14.13. MS (ESI-TOF) for $C_{13}H_{19}N_3$ $[M + H]^+$ calculated 218.1652, found 218.1706.

*1-Benzyl-1H-benzo[d]imidazol-2-amine (**8d**).* Benzyl bromide was used as reagent. White solid (28 mg, 63%). R_f = 0.44 (20% MeOH/CH_2Cl_2). ^{1}H NMR (500 MHz, DMSO) δ 7.33−7.28 (m, 2H), 7.24 (ddd, J = 6.4, 3.9, 1.3 Hz, 1H), 7.21−7.16 (m, 2H), 7.13 (d, J = 7.4 Hz, 1H), 7.04 (d, J = 7.4 Hz, 1H), 6.91 (td, J = 7.6, 1.2 Hz, 1H), 6.81 (td, J = 7.6, 1.1 Hz, 1H), 6.52 (s, 2H), 5.25 (s, 2H). ^{13}C NMR (126 MHz, DMSO) δ 155.02, 142.92, 137.25, 134.17, 128.52, 127.27, 127.00, 120.47, 118.06, 114.77, 107.90, 44.66. MS (ESI-TOF) for $C_{14}H_{13}N_3$ calculated $[M + H]^+$ 224.1182, found 224.1183.

*3-((2-Amino-1H-benzo[d]imidazol-1-yl)methyl)benzonitrile (**8e**).* 3-Cyanobenzyl bromide was used as reagent. White solid (38 mg, 76%). R_f = 0.40 (20% MeOH/CH_2Cl_2). ^{1}H NMR (500 MHz, $CDCl_3$) δ 7.61 (d, J = 7.7 Hz, 1H), 7.51−7.47 (m, 2H), 7.45 (d, J = 7.7 Hz, 1H), 7.39−7.35 (m, 1H), 7.19 (td, J = 7.7, 1.2 Hz, 1H), 7.09 (td, J = 7.6, 1.1 Hz, 1H), 7.03 (d, J = 7.5 Hz, 1H), 5.19 (s, 2H), 4.62 (bs, 2H). ^{13}C NMR (126 MHz, $CDCl_3$) δ 153.12, 141.95, 137.21, 134.26, 132.07, 130.90, 130.28, 130.09, 122.42, 120.72, 118.27, 117.25, 113.59, 107.81, 45.56. MS (ESI-TOF) for $C_{15}H_{12}N_4$ $[M + H]^+$ calculated 249.1135, found 249.1136.

*1-(3-(Aminomethyl)benzyl)-1H-benzo[d]imidazol-2-amine (**8f**).* To a solution of compound **8e** (25 mg, 0.1 mmol) in THF (2 mL) was added $LiAlH_4$ (0.4 mL, 0.4 mmol, 1.0 M inTHF) at 0 °C under nitrogen atmosphere. The reaction mixture was stirred for 1 h at 25 °C and 5 h at 75 °C. The reaction mixture was cooled to room temperature and quenched carefully with ice-cold water. The resulting mixture was basified with 10% NaOH (to pH = 8.0) and extracted with CH_2Cl_2 (3 × 10 mL). The combined organic layer was dried over Na_2SO_4 and concentrated under reduced pressure, and the crude material was purified by neutral-alumina column chromatography (30% MeOH/CH_2Cl_2) to obtain the compound **8f** as a white solid (17 mg, 67%). R_f = 0.20 (40% MeOH/CH_2Cl_2). ^{1}H NMR (400 MHz, DMSO) δ 7.25−7.20 (m, 3H), 7.12 (d, J = 7.7 Hz, 1H), 7.02 (d, J = 7.4 Hz, 1H), 7.00−6.95 (m, 1H), 6.91 (td, J = 7.6, 1.1 Hz, 1H), 6.80 (td, J = 7.6, 1.0 Hz, 1H), 6.50 (s, 2H), 5.22 (s, 2H), 3.67 (s, 2H). ^{13}C NMR (126 MHz, DMSO) δ 155.03, 144.18, 142.95, 137.02, 134.23, 128.31, 126.09, 125.85, 124.92, 120.42, 118.03, 114.75, 107.92, 45.44, 44.83. MS (ESI-TOF) for $C_{15}H_{16}N_4$ $[M + H]^+$ calculated 253.1448, found 253.1470.

*Butyl 2-amino-1H-benzo[d]imidazole-1-carboxylate (**9**).* To a solution of 2-aminobenzimidazole (**7**) (27 mg, 0.2 mmol) in anhydrous THF (2 mL) was added butyl chloroformate (27 μL, 0.2 mmol) under nitrogen atmosphere. The reaction mixture was stirred for 3 h. The reaction mixture was diluted with water and extracted with EtOAc (3 × 10 mL). The combined organic layer was dried over Na_2SO_4 and concentrated under reduced pressure, and the crude material was purified by silica gel column chromatography (20% MeOH/CH_2Cl_2) to afford the compound **9** as a white solid (28 mg, 60%). R_f = 0.65 (10% MeOH/CH_2Cl_2). ^{1}H NMR (500 MHz, DMSO) δ 7.60 (d, J = 7.6 Hz, 1H), 7.22 (bs, 2H), 7.18 (dd, J = 7.8, 0.7 Hz, 1H), 7.13 (td, J = 7.6, 1.2 Hz, 1H), 7.05−6.93 (m, 1H), 4.45 (t, J = 6.6 Hz, 2H), 1.86−1.72 (m, 2H), 1.52−1.38 (m, 2H), 0.95 (t, J = 7.4 Hz, 3H). ^{13}C NMR (126 MHz, DMSO) δ 153.58, 151.26, 142.89, 130.02, 124.11, 119.91, 115.54, 113.61, 67.42, 29.94, 18.68, 13.57. MS (ESI-TOF) for $C_{12}H_{15}N_3O_2$ $[M + H]^+$ calculated 234.1237, found 234.1260.

*N-(1-Pentyl-1H-benzo[d]imidazol-2-yl)acetamide(**10**).* To a stirred solution of compound **8b** (41 mg, 0.2 mmol) in pyridine (2 mL) was added acetyl chloride (14 μL, 0.2 mmol). The reaction mixture was stirred for 3 h. The solvent was removed under reduced pressure. The reaction mixture was diluted with water and extracted with EtOAc (3 × 10 mL). The combined organic layer was dried over Na_2SO_4 and concentrated under reduced pressure, and the crude material was purified by silica gel column chromatography (10% MeOH/CH_2Cl_2) to afford the compound **10** as a white solid (32 mg, 65%). R_f = 0.62 (10% MeOH/CH_2Cl_2). ^{1}H NMR (500 MHz, $CDCl_3$) δ 12.19 (bs, 1H), 7.29 (d, J = 8.1 Hz, 1H), 7.25−7.18 (m, 3H), 4.11 (t, J = 7.4 Hz, 2H), 2.24 (s, 3H), 1.87−1.73 (m, 2H), 1.45−1.30 (m, 4H), 0.90 (t, J = 7.0 Hz, 3H). ^{13}C NMR (126 MHz, $CDCl_3$) δ 183.60, 153.38, 129.66, 128.46, 123.01, 122.89, 111.34, 109.47, 42.07, 29.85, 28.92, 28.12, 22.42, 14.08. MS (ESI-TOF) for $C_{14}H_{19}N_3O$ $[M + H]^+$ calculated 246.1601, found 246.1637.

Compound **12** was synthesized similarly as compound **7**.

*1H-Naphtho[2,3-d]imidazol-2-amine (**12**).* Naphthalene-2,3-diamine was used as reagent. Off-white solid (135 mg, 74%). R_f = 0.35 (20% MeOH/CH_2Cl_2). ^{1}H NMR (500 MHz, DMSO) δ 10.78 (bs, 1H), 7.77 (dd, J = 6.2, 3.3 Hz, 2H), 7.47 (s, 2H), 7.20 (dd, J = 6.3, 3.3 Hz, 2H), 6.60 (s, 2H). ^{13}C NMR (126 MHz, DMSO) δ 158.41, 129.03, 126.87, 126.81, 121.99, 106.25. MS (ESI-TOF) for $C_{11}H_9N_3$ $[M + H]^+$ calculated 184.0869, found 184.0877.

Compound **13** was synthesized similarly as compound **8a**.

*1-Pentyl-1H-naphtho[2,3-d]imidazol-2-amine (**13**).* Compound **12** was used as reagent. Off-white solid (40 mg, 79%). R_f = 0.45 (10% MeOH/CH_2Cl_2). ^{1}H NMR (500 MHz, DMSO) δ 7.85−7.77 (m, 2H), 7.53 (s, 1H), 7.52 (s, 1H), 7.27−7.21 (m, 2H), 6.97 (s, 2H), 4.05 (t, J = 7.3 Hz, 2H), 1.75−1.64 (m, 2H), 1.36−1.27 (m, 4H), 0.85 (t, J = 6.9 Hz, 3H). ^{13}C NMR (126 MHz, DMSO) δ 157.56, 135.95, 129.84, 128.17, 126.97, 126.91, 122.45, 122.13, 109.25, 102.56, 41.58, 28.32, 27.85, 21.99, 13.98. MS (ESI-TOF) for $C_{16}H_{19}N_3$ $[M + H]^+$ calculated 254.1652, found 254.1714.

*1-Methoxy-2-nitronaphthalene (**15**).* To a solution of compound 2-nitro-1-naphthol (189 mg, 1 mmol) in acetone (5 mL) were added KOH (168 mg, 3 mmol) and MeI (124 μL, 2 mmol). The reaction mixture was refluxed for 12 h. The reaction mixture was cooled to room temperature, and solvent was removed under reduced pressure. Water was then added to the reaction mixture and extracted with EtOAc (3 × 30 mL). The combined organic layer was dried over Na_2SO_4 and concentrated under reduced pressure, and the crude material was purified by silica gel column chromatography (10% EtOAc/hexanes) to obtain the compound **15** as a pale yellow solid (178 mg, 88%). R_f = 0.50 (10% EtOAc/hexanes). ^{1}H NMR (500 MHz, $CDCl_3$) δ 8.32 (ddd, J = 3.0, 1.6, 0.7 Hz, 1H), 7.90 (d, J = 8.9 Hz, 2H), 7.71−7.60 (m, 3H), 4.15 (s, 3H). ^{13}C NMR (126 MHz, $CDCl_3$) δ 151.85, 139.19, 136.61, 129.61, 128.70, 128.34, 127.74, 124.49, 124.30, 121.16, 63.88.

*2-Nitro-N-pentylnaphthalen-1-amine (**16**).* To a solution of compound **15** (102 mg, 0.5 mmol) in DMF (3 mL) was added amyl amine (87 μL, 0.75 mmol). The reaction mixture was stirred for 10 h at 60 °C. The reaction mixture was diluted with water and extracted with EtOAc (3 × 20 mL). The combined organic layer was dried over Na_2SO_4 and concentrated under reduced pressure, and the crude material was purified by silica gel column chromatography (10% EtOAc/hexanes) to obtain the compound **16** as a red solid (115 mg, 89%). R_f = 0.62 (10% EtOAc/hexanes). ^{1}H NMR (500 MHz, $CDCl_3$) δ 9.01 (bs, 1H), 8.31 (d, J = 8.5 Hz, 1H), 8.08 (d, J = 9.3 Hz, 1H), 7.77−7.70 (m, 1H), 7.60 (ddd, J = 8.1, 6.9, 1.1 Hz, 1H), 7.46 (ddd, J = 8.4, 6.9, 1.4 Hz, 1H), 7.10 (d, J = 9.3 Hz, 1H), 3.77 (td, J = 7.0, 5.3 Hz, 2H), 1.79−1.67 (m, 2H), 1.46−1.28 (m, 4H), 0.90 (t, J = 7.1 Hz, 3H). ^{13}C NMR (126 MHz, $CDCl_3$) δ 149.00, 138.03, 130.98, 130.18, 128.60, 128.10, 125.92, 125.25, 121.89, 118.44, 51.31, 31.63, 29.09, 22.46, 14.07. MS (ESI-TOF) for $C_{15}H_{18}N_2O_2$ $[M + H]^+$ calculated 259.1441, found 259.1386.

*1-Pentyl-1H-naphtho[1,2-d]imidazol-2-amine (**18**).* To a solution of compound **16** (52 mg, 0.2 mmol) in anhydrous EtOAc (5 mL) was added a catalytic amount of 5% Pt on carbon (16 mg, 2 mol %). The reaction mixture was subjected to hydrogenation at 30 psi H_2 pressure for 3 h. The reaction mixture was filtered, and the filtrate was concentrated under the reduced pressure to obtain compound **17**. To a solution of compound **17** in a 1:1 mixture of MeOH (1 mL) and water (1 mL) was added CNBr (64 mg, 0.6 mmol). The reaction mixture was stirred for 3 h at 60 °C. The reaction mixture was cooled to room temperature, and MeOH removed under reduced pressure. The remaining mixture was basified with 1.0 M aq. NaOH (to pH = 8.0) and extracted with EtOAc (3 × 10 mL). The combined organic layer was dried over Na_2SO_4 and concentrated under reduced pressure, and the crude material was purified by silica gel column chromatography (10% MeOH/CH_2Cl_2) to obtain the compound **18** as a purple solid (35 mg, 69%). R_f = 0.45 (10% MeOH/CH_2Cl_2). ^{1}H NMR (500 MHz, $CDCl_3$) δ 8.08 (d, J = 8.5 Hz, 1H), 7.94 (d, J = 7.5 Hz, 1H), 7.69−7.59 (m, 2H), 7.52 (ddd, J = 8.4, 6.9, 1.3 Hz, 1H), 7.38 (ddd, J = 8.0, 6.9, 1.0 Hz, 1H), 4.76 (bs, 2H), 4.35 (t, J = 7.6 Hz, 2H), 2.05−1.92 (m, 2H), 1.53−1.43 (m, 2H), 1.43−1.36 (m, 2H), 0.93 (t, J = 7.2 Hz, 3H). ^{13}C NMR (126 MHz, $CDCl_3$) δ 152.28, 138.22, 130.26, 129.91, 126.14, 125.95, 123.19, 122.84, 121.52, 118.84, 118.07, 45.55, 29.62, 29.19, 22.57, 14.12. MS (ESI-TOF) for $C_{16}H_{19}N_3$ $[M + H]^+$ calculated 254.1652, found 254.1715.

Compound **20** was synthesized similarly as compound **15**.

*2-Methoxy-1-nitronaphthalene (**20**).* 1-Nitro-2-naphthol was used as reagent. Green solid (164 mg, 81%). R_f = 0.50 (10% EtOAc/hexanes). ^{1}H NMR (500 MHz, $CDCl_3$) δ 7.97 (d, J = 9.1 Hz, 1H), 7.85 (d, J = 8.3 Hz, 1H), 7.68 (dd, J = 8.6, 0.8 Hz, 1H), 7.63−7.57 (m, 1H), 7.49−7.42 (m, 1H), 7.35 (d, J = 9.2 Hz, 1H), 4.04 (s, 3H). ^{13}C NMR (126 MHz, $CDCl_3$) δ 148.76, 132.33, 129.30, 128.35, 128.18, 125.83, 125.31, 120.59, 113.19, 57.21.

Compound **21** was synthesized similarly as compound **16**.

*1-Nitro-N-pentylnaphthalen-2-amine (**21**).* Compound **20** was used as reagent. Orange solid (102 mg, 79%). R_f = 0.60 (10% EtOAc/hexanes). ^{1}H NMR (500 MHz, $CDCl_3$) δ 8.94 (bs, 1H), 8.79 (d, J = 8.8 Hz, 1H), 7.79 (d, J = 9.4 Hz, 1H), 7.67 (dd, J = 7.9, 1.3 Hz, 1H), 7.60 (ddd, J = 8.6, 7.0, 1.5 Hz, 1H), 7.33 (ddd, J = 7.9, 7.1, 1.0 Hz, 1H), 7.07 (d, J = 9.3 Hz, 1H), 3.44 (td, J = 7.1, 5.4 Hz, 2H), 1.83−1.73 (m, 2H), 1.51−1.35 (m, 4H), 0.94 (t, J = 7.2 Hz, 3H). ^{13}C NMR (126 MHz, $CDCl_3$) δ 146.99, 137.46, 130.37, 129.11, 128.89, 126.47, 125.56, 124.03, 123.44, 114.23, 43.71, 29.26, 29.14, 22.52, 14.11. MS (ESI-TOF) for $C_{15}H_{18}N_2O_2$ $[M + H]^+$ calculated 259.1441, found 259.1384.

Compound **23** was synthesized similarly as compound **18**.

*3-Pentyl-3H-naphtho[1,2-d]imidazol-2-amine (**23**).* Compound **21** was used as reagent. Purple solid (37 mg, 73%). R_f = 0.45 (10% MeOH/CH_2Cl_2). ^{1}H NMR (500 MHz, DMSO) δ 8.18 (d, J = 8.3 Hz, 1H), 7.85 (d, J = 8.2 Hz, 1H), 7.48 (d, J = 8.6 Hz, 1H), 7.44−7.40 (m, 2H), 7.31 (ddd, J = 8.1, 6.8, 1.3 Hz, 1H), 6.42 (s, 2H), 4.08 (t, J = 7.2 Hz, 2H), 1.75−1.63 (m, 2H), 1.35−1.16 (m, 4H), 0.83 (t, J = 6.9 Hz, 3H). ^{13}C NMR (126 MHz, DMSO) δ 153.77, 136.96, 129.24, 129.19, 128.18, 124.60, 124.58, 122.75, 121.13, 117.88, 109.93, 41.60, 28.56, 28.29, 21.95, 13.95. MS (ESI-TOF) for $C_{16}H_{19}N_3$ $[M + H]^+$ calculated 254.1652, found 254.1713.

*2-Nitro-N-pentylpyridin-3-amine (**25a**).* To a solution of compound 3-fluoro-2-nitropyridine (142 mg, 1 mmol) in DMSO (2 mL) were added amyl amine (116 μL, 1 mmol) and DIPEA (174 μL, 1 mmol). The reaction mixture was stirred for 6 h at 60 °C. After the completion of the reaction (monitored by TLC), the reaction mixture was diluted with water and extracted with EtOAc (3 × 20 mL). The combined organic layer was dried over Na_2SO_4 and concentrated under reduced pressure, and the crude material was purified by flash chromatography (10% EtOAc/hexanes) to afford the compound **25a** as a yellow oil (184 mg, 88%). R_f = 0.30 (10% EtOAc/hexanes). ^{1}H NMR (500 MHz, $CDCl_3$) δ 7.88 (dd, J = 1.43, 3.96 Hz, 1H), 7.75 (s, 1H), 7.43 (ddd, J = 0.62, 3.96, 8.59 Hz, 1H), 7.33 (dd, J = 1.29, 8.62 Hz, 1H), 3.29 (td, J = 5.29, 7.12 Hz, 2H), 1.79−1.68 (m, 2H), 1.48−1.31 (m, 4H), 0.93 (t, J = 7.12 Hz, 3H). ^{13}C NMR (126 MHz, $CDCl_3$) δ 141.21, 140.82, 135.10, 130.58, 123.44, 42.92, 29.26, 28.67, 22.48, 14.09. MS (ESI-TOF) for $C_{10}H_{15}N_3O_2$ $[M + H]^+$ calculated 210.1237, found 210.1214.

Compounds **25b**−**25d** were synthesized similarly as compound **25a**.

*3-Nitro-N-pentylpyridin-4-amine (**25b**).* 4-Chloro-3-nitropyridine was used as reagent. Yellow oil (179 mg, 86%). R_f = 0.20 (10% EtOAc/hexanes). ^{1}H NMR (500 MHz, $CDCl_3$) δ 9.20 (s, 1H), 8.28 (dd, J = 6.2, 0.7 Hz, 1H), 8.16 (bs, 1H), 6.70 (d, J = 6.2 Hz, 1H), 3.32 (td, J = 7.2, 5.4 Hz, 2H), 1.79−1.69 (m, 2H), 1.47−1.32 (m, 4H), 0.94 (t, J = 7.1 Hz, 3H). ^{13}C NMR (126 MHz, $CDCl_3$) δ 153.22, 149.30, 148.82, 129.79, 107.87, 42.92, 29.18, 28.50, 22.44, 14.06. MS (ESI-TOF) for $C_{10}H_{15}N_3O_2$ $[M + H]^+$ calculated 210.1237, found 210.1307.

*4-Nitro-N-pentylpyridin-3-amine (**25c**).* 3-Fluoro-4-nitropyridine was used as reagent. Yellow solid (184 mg, 88%). R_f = 0.20 (10% EtOAc/hexanes). ^{1}H NMR (500 MHz, $CDCl_3$) δ 8.15 (d, J = 8.9 Hz, 1H), 7.86 (d, J = 2.9 Hz, 1H), 6.91 (dd, J = 9.0, 2.9 Hz, 1H), 3.23 (t, J = 7.2 Hz, 2H), 1.73−1.64 (m, 2H), 1.45−1.34 (m, 4H), 0.93 (t, J = 7.1 Hz, 3H). ^{13}C NMR (126 MHz, $CDCl_3$) δ 148.64, 147.60, 133.24, 120.64, 117.58, 43.46, 29.18, 28.77, 22.50, 14.09. MS (ESI-TOF) for $C_{10}H_{15}N_3O_2$ $[M + H]^+$ calculated 210.1237, found 210.1197.

*3-Nitro-N-pentylpyridin-2-amine (**25d**).* 2-Chloro-3-nitropyridine was used as reagent. Yellow oil (188 mg, 90%). R_f = 0.22 (10% EtOAc/hexanes). ^{1}H NMR (500 MHz, $CDCl_3$) δ 8.43−8.38 (m, 2H), 8.25 (bs, 1H), 6.62 (dd, J = 8.0, 4.8 Hz, 1H), 3.65−3.58 (m, 2H), 1.74−1.64 (m, 2H), 1.46−1.33 (m, 4H), 0.92 (t, J = 7.1 Hz, 3H). ^{13}C NMR (126 MHz, $CDCl_3$) δ 156.02, 152.91, 135.45, 128.01, 111.55, 41.46, 29.34, 29.20, 22.56, 14.15. MS (ESI-TOF) for $C_{10}H_{15}N_3O_2$ $[M + H]^+$ calculated 210.1237, found 210.1220.

Compounds **27a**−**27d** were synthesized similarly as compound **18**.

*1-Pentyl-1H-imidazo[4,5-b]pyridin-2-amine (**27a**).* Compound **25a** was used as reagent. White solid (29 mg, 71%). R_f = 0.42 (10% MeOH/CH_2Cl_2). ^{1}H NMR (500 MHz, DMSO) δ 7.94 (dd, J = 5.0, 1.3 Hz, 1H), 7.42 (dd, J = 7.6, 1.4 Hz, 1H), 6.86 (bs, 2H), 6.81 (dd, J = 7.6, 5.0 Hz, 1H), 3.96 (t, J = 7.2 Hz, 2H), 1.65−1.56 (m, 2H), 1.32−1.17 (m, 4H), 0.83 (t, J = 7.1 Hz, 3H). ^{13}C NMR (126 MHz, DMSO) δ 156.80, 156.50, 140.62, 126.91, 113.48, 113.42, 41.32, 28.22, 28.09, 21.91, 13.93. MS (ESI-TOF) for $C_{11}H_{16}N_4$ $[M + H]^+$ calculated 205.1448, found 205.1491.

*1-Pentyl-1H-imidazo[4,5-c]pyridin-2-amine (**27b**).* Compound **25b** was used as reagent. White solid (29 mg, 71%). R_f = 0.20 (10% MeOH/CH_2Cl_2). ^{1}H NMR (500 MHz, DMSO) δ 8.33 (s, 1H), 8.01 (d, J = 5.21 Hz, 1H), 7.19 (d, J = 5.17 Hz, 1H), 6.73 (s, 2H), 3.98 (t, J = 7.21 Hz, 2H), 1.67−1.55 (m, 2H), 1.34−1.14 (m, 4H), 0.83 (t, J = 7.12 Hz, 3H). ^{13}C NMR (126 MHz, DMSO) δ 155.64, 140.08, 139.51, 138.55, 135.79, 103.52, 41.57, 28.19, 28.08, 21.88, 13.92. MS (ESI-TOF) for $C_{11}H_{16}N_4$ $[M + H]^+$ calculated 205.1448, found 205.1477.

*3-Pentyl-3H-imidazo[4,5-c]pyridin-2-amine (**27c**).* Compound **25c** was used as reagent. White solid (30 mg, 74%). R_f = 0.40 (10% MeOH/CH_2Cl_2). ^{1}H NMR (500 MHz, DMSO) δ 7.84 (d, J = 2.6 Hz, 1H), 7.32 (dd, J = 8.9, 3.0 Hz, 1H), 6.48 (dd, J = 8.9, 0.5 Hz, 1H), 5.98 (s, 2H), 3.47 (t, J = 7.1 Hz, 2H), 1.64−1.56 (m, 2H), 1.38−1.26 (m, 4H), 0.87 (t, J = 7.1 Hz, 3H). ^{13}C NMR (126 MHz, DMSO) δ 157.42, 138.53, 129.16, 126.49, 114.87, 108.44, 50.58, 27.89, 26.70, 21.71, 13.86. MS (ESI-TOF) for $C_{11}H_{16}N_4$ $[M + H]^+$ calculated 205.1448, found 205.1495.

*3-Pentyl-3H-imidazo[4,5-b]pyridin-2-amine (**27d**).* Compound **25d** was used as reagent. White solid (34 mg, 83%). R_f = 0.45 (10% MeOH/CH_2Cl_2). ^{1}H NMR (500 MHz, DMSO) δ 7.83 (dd, J = 5.0, 1.4 Hz, 1H), 7.37 (dd, J = 7.7, 1.4 Hz, 1H), 6.93 (dd, J = 7.7, 5.0 Hz, 1H), 6.75 (s, 2H), 4.00 (t, J = 7.3 Hz, 2H), 1.70−1.60 (m, 2H), 1.34−1.19 (m, 4H), 0.83 (t, J = 7.1 Hz, 3H). ^{13}C NMR (126 MHz, DMSO) δ 155.48, 147.91, 137.37, 135.70, 119.96, 116.61, 40.06, 28.26, 28.00, 21.85, 13.92. MS (ESI-TOF) for $C_{11}H_{16}N_4$ $[M + H]^+$ calculated 205.1448, found 205.1470.

Compounds **29a**−**29i** were synthesized similarly as compound **25a**.

*3-Methyl-2-nitro-N-pentylaniline (**29a**).* 1-Fluoro-3-methyl-2-nitrobenzene was used as reagent. Red oil (200 mg, 90%). R_f = 0.70 (10% EtOAc/hexanes). ^{1}H NMR (500 MHz, $CDCl_3$) δ 7.25−7.14 (m, 1H), 6.65 (d, J = 8.5 Hz, 1H), 6.60 (bs, 1H), 6.50 (d, J = 7.4 Hz, 1H), 3.19 (td, J = 7.1, 5.1 Hz, 2H), 2.47 (s, 3H), 1.73−1.60 (m, 2H), 1.46−1.31 (m, 4H), 0.92 (t, J = 7.1 Hz, 3H). ^{13}C NMR (126 MHz, $CDCl_3$) δ 144.34, 135.92, 135.59, 133.41, 119.09, 111.31, 43.55, 29.36, 28.86, 22.55, 21.71,

dx.doi.org/10.1021/jm500701q | J. Med. Chem. 2014, 57, 7325−7341

14.13. MS (ESI-TOF) for $C_{12}H_{18}N_2O_2$ $[M + H]^+$ calculated 223.1441, found 223.1400.

*4-Methyl-2-nitro-N-pentylaniline (**29b**).* 1-Fluoro-4-methyl-2-nitrobenzene was used as reagent. Red oil (180 mg, 81%). R_f = 0.65 (10% EtOAc/hexanes). ^{1}H NMR (500 MHz, $CDCl_3$) δ 8.02−7.91 (m, 2H), 7.27−7.24 (m, 1H), 6.76 (d, J = 8.8 Hz, 1H), 3.28 (td, J = 7.1, 5.3 Hz, 2H), 2.26 (s, 3H), 1.78−1.66 (m, 2H), 1.47−1.34 (m, 4H), 0.93 (t, J = 7.1 Hz, 3H). ^{13}C NMR (126 MHz, $CDCl_3$) δ 144.12, 137.93, 131.39, 126.20, 124.67, 113.93, 43.22, 29.37, 28.86, 22.54, 20.11, 14.13. MS (ESI-TOF) for $C_{12}H_{18}N_2O_2$ $[M + H]^+$ calculated 223.1441, found 223.1410.

*5-Methyl-2-nitro-N-pentylaniline (**29c**).* 2-Chloro-4-methyl-1-nitrobenzene was used as reagent. Orange solid (180 mg, 81%). R_f = 0.68 (10% EtOAc/hexanes). ^{1}H NMR (400 MHz, $CDCl_3$) δ 8.11 (bs, 1H), 8.08 (d, J = 8.8 Hz, 1H), 6.63 (s, 1H), 6.46 (dd, J = 8.8, 1.6 Hz, 1H), 3.30 (td, J = 7.1, 5.3 Hz, 2H), 2.36 (s, 3H), 1.83−1.66 (m, 2H), 1.52−1.35 (m, 4H), 0.96 (t, J = 7.1 Hz, 3H). ^{13}C NMR (126 MHz, $CDCl_3$) δ 147.85, 145.86, 129.96, 126.99, 116.96, 113.47, 43.12, 29.37, 28.79, 22.52, 22.35, 14.13. MS (ESI-TOF) for $C_{12}H_{18}N_2O_2$ $[M + H]^+$ calculated 223.1441, found 223.1400.

*2-Methyl-6-nitro-N-pentylaniline (**29d**).* 2-Chloro-1-methyl-3-nitrobenzene was used as reagent. Red oil (175 mg, 79%). R_f = 0.70 (10% EtOAc/hexanes). ^{1}H NMR (500 MHz, $CDCl_3$) δ 7.97−7.86 (m, 1H), 7.28 (ddd, J = 7.3, 1.6, 0.8 Hz, 1H), 6.96 (bs, 1H), 6.74 (dd, J = 8.4, 7.3 Hz, 1H), 3.24 (t, J = 7.2 Hz, 2H), 2.39 (s, 3H), 1.62−1.53 (m, 2H), 1.34−1.31 (m, 4H), 0.89 (t, J = 7.1 Hz, 3H). ^{13}C NMR (126 MHz, $CDCl_3$) δ 146.08, 138.52, 137.93, 130.14, 124.44, 118.36, 48.02, 30.93, 29.13, 22.53, 20.93, 14.11. MS (ESI-TOF) for $C_{12}H_{18}N_2O_2$ $[M + H]^+$ calculated 223.1441, found 223.1445.

*3-Methoxy-2-nitro-N-pentylaniline (**29e**).* 1-Fluoro-3-methoxy-2-nitrobenzene was used as reagent. Red oil (200 mg, 84%). R_f = 0.62 (10% EtOAc/hexanes). ^{1}H NMR (500 MHz, $CDCl_3$) δ 7.22 (dd, J = 12.5, 4.3 Hz, 1H), 6.36 (d, J = 8.6 Hz, 1H), 6.24 (dd, J = 8.2, 0.8 Hz, 1H), 6.19 (bs, 1H), 3.87 (s, 3H), 3.17 (td, J = 7.1, 5.2 Hz, 2H), 1.70−1.61 (m, 2H), 1.42−1.32 (m, 4H), 0.92 (t, J = 7.1 Hz, 3H). ^{13}C NMR (126 MHz, $CDCl_3$) δ 155.44, 144.62, 133.74, 127.24, 105.23, 99.34, 56.57, 43.60, 29.31, 28.89, 22.54, 14.12. MS (ESI-TOF) for $C_{12}H_{18}N_2O_3$ $[M + H]^+$ calculated 239.1390, found 239.1362.

*3-Fluoro-2-nitro-N-pentylaniline (**29f**).* 1, 3-Difluoro-2-nitrobenzene was used as reagent. Red oil (169 mg, 75%). R_f = 0.62 (5% EtOAc/hexanes). ^{1}H NMR (500 MHz, $CDCl_3$) δ 7.31−7.27 (m, 1H), 7.25 (bs, 1H), 6.57 (d, J = 8.8 Hz, 1H), 6.40 (ddd, J = 11.5, 8.1, 1.2 Hz, 1H), 3.23 (td, J = 7.1, 5.2 Hz, 2H), 1.76−1.65 (m, 2H), 1.47−1.33 (m, 4H), 0.93 (t, J = 7.1 Hz, 3H). ^{13}C NMR (126 MHz, $CDCl_3$) δ 158.08 (d, J = 261.9 Hz), 145.85, 134.70 (d, J = 12.0 Hz), 108.71 (d, J = 3.7 Hz), 103.08, 102.90, 43.58, 29.14, 28.57, 22.36, 13.96. MS (ESI-TOF) for $C_{11}H_{15}FN_2O_2$ $[M + H]^+$ calculated 227.1190, found 227.1135.

*3-Chloro-2-nitro-N-pentylaniline (**29g**).* 1-Chloro-3-fluoro-2-nitrobenzene was used as reagent. Orange solid (200 mg, 83%). R_f = 0.65 (5% EtOAc/hexanes). ^{1}H NMR (500 MHz, $CDCl_3$) δ 7.21 (ddd, J = 8.5, 7.9, 0.5 Hz, 1H), 6.71 (ddd, J = 18.3, 8.3, 1.0 Hz, 2H), 5.83 (bs, 1H), 3.17 (td, J = 7.1, 5.2 Hz, 2H), 1.73−1.58 (m, 2H), 1.54−1.22 (m, 4H), 0.92 (t, J = 7.1 Hz, 3H). ^{13}C NMR (126 MHz, $CDCl_3$) δ 144.10, 134.65, 132.91, 128.81, 118.17, 111.83, 43.67, 29.25, 28.78, 22.51, 14.10. MS (ESI-TOF): for $C_{11}H_{15}ClN_2O_2$ $[M + H]^+$ calculated 243.0895, found 243.0841.

*2-Nitro-N-pentyl-3-(trifluoromethyl)aniline (**29h**).* 1-Chloro-2-nitro-3-(trifluoromethyl) benzene was used as reagent. Orange solid (179 mg, 65%). R_f = 0.70 (5% EtOAc/hexanes). ^{1}H NMR (500 MHz, $CDCl_3$) δ 7.41 (dd, J = 8.5, 7.8 Hz, 1H), 7.01 (d, J = 8.1 Hz, 2H), 5.94 (bs, 1H), 3.20 (td, J = 7.1, 5.2 Hz, 2H), 1.74−1.59 (m, 2H), 1.44−1.31 (m, 4H), 0.93 (t, J = 7.1 Hz, 3H). ^{13}C NMR (126 MHz, $CDCl_3$) δ 142.94, 133.02, 132.67, 125.97 (q, J = 32.78 Hz), 122.69 (q, J = 273.57 Hz), 117.43, 114.82 (q, J = 5.71 Hz), 43.67, 29.22, 28.76, 22.50, 14.09. MS (ESI-TOF) for $C_{12}H_{15}F_3N_2O_2$ $[M + H]^+$ calculated 277.1158, found 277.1105.

*3-Bromo-2-nitro-N-pentylaniline (**29i**).* 1-Bromo-3-fluoro-2-nitrobenzene was used as reagent. Orange solid (250 mg, 87%). R_f = 0.70 (5% EtOAc/hexanes). ^{1}H NMR (500 MHz, $CDCl_3$) δ 7.13 (ddd, J = 8.5, 7.9, 0.5 Hz, 1H), 6.92 (dd, J = 7.8, 1.1 Hz, 1H), 6.73 (dd, J = 8.6, 0.8 Hz, 1H), 5.74 (bs, 1H), 3.17 (td, J = 7.1, 5.2 Hz, 2H), 1.74−1.59 (m, 2H), 1.46−1.27 (m, 4H), 0.92 (t, J = 7.1 Hz, 3H). ^{13}C NMR (126 MHz, $CDCl_3$) δ 143.98, 136.28, 133.15, 121.52, 116.46, 112.50, 43.65, 29.24, 28.78, 22.51, 14.10. MS (ESI-TOF) for $C_{11}H_{15}BrN_2O_2$ $[M + H]^+$ calculated 287.0390, found 287.0330.

*3-Ethyl-2-nitro-N-pentylaniline (**29j**).* To a stirred solution of compound **29i** (144 mg, 0.5 mmol) in 1,4-dioxane (3 mL) were added ethylboronic acid (56 mg, 0.75 mmol), $Pd(dppf)Cl_2$ (36 mg, 0.05 mmol), and K_2CO_3 (207 mg, 1.5 mmol). The resulting reaction mixture was stirred at 90 °C under nitrogen atmosphere for 12 h. The reaction mixture was diluted with water and extracted with EtOAc (3 × 20 mL). The combined organic layer was dried over Na_2SO_4 and concentrated under reduced pressure, and crude material was purified by flash chromatography (10% EtOAc/hexanes) to obtain the compound **29j** as a red oil (72 mg, 61%). R_f = 0.70 (10% EtOAc/hexanes). ^{1}H NMR (500 MHz, $CDCl_3$) δ 7.23 (d, J = 8.0 Hz, 1H), 6.67−6.61 (m, 1H), 6.57−6.52 (m, 1H), 6.15 (bs, 1H), 3.17 (td, J = 7.1, 5.1 Hz, 2H), 2.76 (q, J = 7.5 Hz, 2H), 1.74−1.60 (m, 2H), 1.52−1.34 (m, 4H), 1.24 (t, J = 7.5 Hz, 3H), 0.92 (t, J = 7.1 Hz, 3H). ^{13}C NMR (126 MHz, $CDCl_3$) δ 143.50, 141.04, 136.04, 133.22, 117.65, 111.07, 43.60, 29.36, 28.90, 27.09, 22.56, 15.25, 14.13. MS (ESI-TOF) for $C_{13}H_{20}N_2O_2$ $[M + H]^+$ calculated 237.1598, found 237.1581.

*N,N-Dimethyl-2-nitro-N′-pentyl-benzene-1,3-diamine (**29k**).* To a solution of compound **29g** (242 mg, 1 mmol) in DMF (3 mL) was added dimethyl amine (2 mL, 4 mmol, 2.0 M in MeOH). The reaction mixture was stirred for 12 h at 75 °C. The reaction mixture was cooled to room temperature, diluted with water, and extracted with EtOAc (3 × 30 mL). The combined organic layer was dried over Na_2SO_4 and concentrated under reduced pressure, and the crude material was purified by silica gel column chromatography (10% EtOAc/hexanes) to obtain the compound **29k** as a red solid (200 mg, 80%). R_f = 0.3 (10% EtOAc/hexanes). ^{1}H NMR (500 MHz, $CDCl_3$) δ 7.19−7.11 (m, 1H), 6.60 (bs, 1H), 6.22−6.11 (m, 2H), 3.16 (td, J = 7.1, 5.1 Hz, 2H), 2.85 (s, 6H), 1.72−1.62 (m, 2H), 1.44−1.31 (m, 4H), 0.92 (t, J = 7.1 Hz, 3H). ^{13}C NMR (126 MHz, $CDCl_3$) δ 149.09, 145.16, 133.87, 126.83, 103.86, 101.81, 43.69, 42.37, 29.38, 28.94, 22.56, 14.14. MS (ESI-TOF) for $C_{13}H_{21}N_3O_2$ $[M + H]^+$ calculated 252.1707, found 252.1734.

Compounds **31a**−**31k** were synthesized similarly as compound **18**.

*4-Methyl-1-pentyl-1H-benzo[d]imidazol-2-amine (**31a**).* Compound **29a** was used as reagent. White solid (33 mg, 76%). R_f = 0.50 (10% MeOH/CH_2Cl_2). ^{1}H NMR (500 MHz, DMSO) δ 6.93 (dd, J = 7.3, 1.2 Hz, 1H), 6.82−6.61 (m, 2H), 6.34 (s, 2H), 3.92 (t, J = 7.2 Hz, 2H), 2.34 (s, 3H), 1.70−1.46 (m, 2H), 1.40−1.10 (m, 4H), 0.83 (t, J = 7.1 Hz, 3H). ^{13}C NMR (126 MHz, DMSO) δ 154.21, 141.56, 133.59, 123.77, 120.83, 117.83, 105.20, 41.44, 28.30, 28.21, 21.95, 16.41, 13.95. MS (ESI-TOF) for $C_{13}H_{19}N_3$ $[M + H]^+$ calculated 218.1652, found 218.1657.

*5-Methyl-1-pentyl-1H-benzo[d]imidazol-2-amine (**31b**).* Compound **29b** was used as reagent. White solid (35 mg, 81%). R_f = 0.47 (10% MeOH/CH_2Cl_2). ^{1}H NMR (500 MHz, DMSO) δ 6.97 (d, J = 7.9 Hz, 1H), 6.91 (s, 1H), 6.67 (dd, J = 7.9, 0.9 Hz, 1H), 6.28 (s, 2H), 3.90 (t, J = 7.2 Hz, 2H), 2.30 (s, 3H), 1.63−1.55 (m, 2H), 1.32−1.18 (m, 4H), 0.83 (t, J = 7.1 Hz, 3H). ^{13}C NMR (126 MHz, DMSO) δ 154.87, 143.08, 132.31, 128.68, 118.76, 115.11, 106.99, 41.35, 28.29, 28.19, 21.94, 21.27, 13.95. MS (ESI-TOF) for $C_{13}H_{19}N_3$ $[M + H]^+$ calculated 218.1652, found 218.1705.

*6-Methyl-1-pentyl-1H-benzo[d]imidazol-2-amine (**31c**).* Compound **29c** was used as reagent. White solid (32 mg, 74%). R_f = 0.44 (10% MeOH/CH_2Cl_2). ^{1}H NMR (500 MHz, DMSO) δ 6.98 (d, J = 7.9 Hz, 1H), 6.91 (s, 1H), 6.72 (dd, J = 7.9, 0.9 Hz, 1H), 6.24 (s, 2H), 3.90 (t, J = 7.3 Hz, 2H), 2.33 (s, 3H), 1.68−1.52 (m, 2H), 1.35−1.15 (m, 4H), 0.85 (t, J = 7.0 Hz, 3H). ^{13}C NMR (126 MHz, DMSO) δ 154.50, 140.65, 134.41, 126.72, 121.05, 114.32, 107.79, 41.30, 28.29, 28.18, 21.94, 21.32, 13.96. MS (ESI-TOF) for $C_{13}H_{19}N_3$ $[M + H]^+$ calculated 218.1652, found 218.1705.

*7-Methyl-1-pentyl-1H-benzo[d]imidazol-2-amine (**31d**).* Compound **29d** was used as reagent. White solid (30 mg, 69%). R_f = 0.45 (10% MeOH/CH_2Cl_2). ^{1}H NMR (500 MHz, DMSO) δ 6.95 (d, J = 7.7 Hz, 1H), 6.79 (t, J = 7.6 Hz, 1H), 6.59 (d, J = 7.3 Hz, 1H), 6.25 (s, 2H), 4.06 (t, J = 7.9 Hz, 2H), 2.52 (s, 3H), 1.76−1.43 (m, 2H),

1.40−1.17 (m, 4H), 0.86 (t, J = 6.9 Hz, 3H). ^{13}C NMR (126 MHz, DMSO) δ 155.09, 143.20, 131.95, 121.27, 120.14, 118.06, 113.16, 42.80, 30.27, 28.12, 21.95, 17.79, 13.99. MS (ESI-TOF) for $C_{13}H_{19}N_3$ $[M + H]^+$ calculated 218.1652, found 218.1707.

*4-Methoxy-1-pentyl-1H-benzo[d]imidazol-2-amine (**31e**).* Compound **29e** was used as reagent. White solid (33 mg, 71%). R_f = 0.40 (10% MeOH/CH_2Cl_2). ^{1}H NMR (500 MHz, DMSO) δ 6.83−6.71 (m, 2H), 6.52 (dd, J = 7.4, 1.5 Hz, 1H), 6.22 (s, 2H), 3.92 (t, J = 7.2 Hz, 2H), 3.86 (s, 3H), 1.70−1.49 (m, 2H), 1.37−1.18 (m, 4H), 0.83 (t, J = 7.1 Hz, 3H). ^{13}C NMR (126 MHz, DMSO) δ 153.50, 148.20, 135.74, 131.77, 118.49, 104.14, 101.46, 55.90, 41.55, 28.28, 28.17, 21.93, 13.95. MS (ESI-TOF) for $C_{13}H_{19}N_3O$ $[M + H]^+$ calculated 234.1601, found 234.1619.

*4-Fluoro-1-pentyl-1H-benzo[d]imidazol-2-amine (**31f**).* Compound **29f** was used as reagent. White solid (35 mg, 79%). R_f = 0.50 (10% MeOH/CH_2Cl_2). ^{1}H NMR (500 MHz, DMSO) δ 6.98 (d, J = 7.8 Hz, 1H), 6.86−6.78 (m, 1H), 6.78−6.69 (m, 1H), 6.55 (bs, 2H), 3.96 (t, J = 7.2 Hz, 2H), 1.72−1.50 (m, 2H), 1.40−1.15 (m, 4H), 0.83 (t, J = 7.0 Hz, 3H). ^{13}C NMR (126 MHz, DMSO) δ 155.05, 150.78 (d, J = 243.6 Hz), 137.50 (d, J = 10.8 Hz), 130.24 (d, J = 16.0 Hz), 118.09 (d, J = 7.2 Hz), 106.36 (d, J = 17.9 Hz), 104.18 (d, J = 2.9 Hz). 41.75, 28.23, 28.06, 21.91, 13.93. MS (ESI-TOF) for $C_{12}H_{16}FN_3$ $[M + H]^+$ calculated 222.1401, found 222.1451.

*4-Chloro-1-pentyl-1H-benzo[d]imidazol-2-amine (**31g**).* Compound **29g** was used as reagent. White solid (35 mg, 74%). R_f = 0.60 (10% MeOH/CH_2Cl_2). ^{1}H NMR (500 MHz, DMSO) δ 7.10 (dd, J = 7.8, 0.9 Hz, 1H), 6.97 (dd, J = 7.9, 0.9 Hz, 1H), 6.90−6.81 (m, 1H), 6.69 (s, 2H), 3.96 (t, J = 7.2 Hz, 2H), 1.75−1.44 (m, 2H), 1.40−1.12 (m, 4H), 0.83 (t, J = 7.1 Hz, 3H). ^{13}C NMR (126 MHz, DMSO) δ 155.48, 139.67, 135.40, 120.05, 118.65, 118.31, 106.55, 41.73, 28.22, 28.06, 21.92, 13.93. MS (ESI-TOF) for $C_{12}H_{16}ClN_3$ $[M + H]^+$ calculated 238.1106, found 238.1160.

*1-Pentyl-4-(trifluoromethyl)-1H-benzo[d]imidazol-2-amine (**31h**).* Compound **29h** was used as a reagent. White solid (38 mg, 70%). R_f = 0.70 (10% MeOH/CH_2Cl_2). ^{1}H NMR (500 MHz, DMSO) δ 7.39 (d, J = 7.8 Hz, 1H), 7.20 (d, J = 7.7 Hz, 1H), 6.97 (t, J = 7.7 Hz, 1H), 6.89 (s, 2H), 4.00 (t, J = 7.3 Hz, 2H), 1.72−1.53 (m, 2H), 1.36−1.19 (m, 4H), 0.84 (t, J = 7.0 Hz, 3H). ^{13}C NMR (126 MHz, DMSO) δ 156.36, 140.33, 135.47, 124.80 (q, J = 271.9 Hz), 117.03, 116.80 (q, J = 4.8 Hz), 113.97 (q, J = 30.9 Hz), 111.21, 41.53, 28.23, 28.10, 21.92, 13.93. MS (ESI-TOF) for $C_{13}H_{16}F_3N_3$ $[M + H]^+$ calculated 272.1369, found 272.1429.

*4-Bromo-1-pentyl-1H-benzo[d]imidazol-2-amine (**31i**).* Compound **29i** was used as reagent. White solid (44 mg, 78%). R_f = 0.68 (10% MeOH/CH_2Cl_2). ^{1}H NMR (500 MHz, DMSO) δ 7.12 (ddd, J = 15.6, 7.8, 0.8 Hz, 2H), 6.80 (t, J = 7.8 Hz, 1H), 6.71 (s, 2H), 3.95 (t, J = 7.2 Hz, 2H), 1.68−1.53 (m, 2H), 1.34−1.06 (m, 4H), 0.83 (t, J = 7.1 Hz, 3H). ^{13}C NMR (126 MHz, DMSO) δ 155.39, 141.17, 134.90, 122.85, 119.13, 107.31, 107.02, 41.76, 28.23, 28.06, 21.92, 13.93. MS (ESI-TOF) for $C_{12}H_{16}BrN_3$ $[M + H]^+$ calculated 282.0600, found 282.0666.

*4-Ethyl-1-pentyl-1H-benzo[d]imidazol-2-amine (**31j**).* Compound **29j** was used as reagent. White solid (35 mg, 76%). R_f = 0.55 (10% MeOH/CH_2Cl_2). ^{1}H NMR (500 MHz, DMSO) δ 6.94 (dd, J = 7.5, 1.4 Hz, 1H), 6.83−6.74 (m, 2H), 6.36 (bs, 2H), 3.92 (t, J = 7.2 Hz, 2H), 2.76 (q, J = 7.6 Hz, 2H), 1.67−1.53 (m, 2H), 1.32−1.24 (m, 4H), 1.21 (t, J = 7.6 Hz, 3H), 0.84 (t, J = 7.0 Hz, 3H). ^{13}C NMR (126 MHz, DMSO) δ 154.11, 140.75, 133.68, 130.17, 119.20, 118.01, 105.30, 41.45, 28.32, 28.23, 23.74, 21.95, 14.81, 13.95. MS (ESI-TOF) for $C_{14}H_{21}N_3$ $[M + H]^+$ calculated 232.1808, found 232.1861.

*N^4,N^4-Dimethyl-1-pentyl-1H-benzo[d]imidazole-2,4-diamine (**31k**).* Compound **29k** was used as reagent. Off-white solid (36 mg, 73%). R_f = 0.5 (20% MeOH/CH_2Cl_2). ^{1}H NMR (500 MHz, DMSO) δ 6.75 (t, J = 7.8 Hz, 1H), 6.65 (dd, J = 7.8, 0.7 Hz, 1H), 6.32−6.26 (m, 1H), 6.18 (bs, 2H), 3.89 (t, J = 7.3 Hz, 2H), 2.98 (s, 6H), 1.65−1.52 (m, 2H), 1.34−1.18 (m, 4H), 0.84 (t, J = 7.0 Hz, 3H). ^{13}C NMR (126 MHz, DMSO) δ 151.95, 140.78, 134.76, 132.60, 118.82, 106.08, 100.09, 41.86, 41.41, 28.32, 28.22, 21.95, 13.96. MS (ESI-TOF) for $C_{14}H_{22}N_4$ $[M + H]^+$ calculated 247.1917, found 247.1950.

*1-Pentyl-4-phenyl-1H-benzo[d]imidazol-2-amine (**31l**).* To a stirred solution of compound **31i** (56 mg, 0.2 mmol) in 1,4-dioxane (2 mL) were added phenylboronic acid (36 mg, 0.3 mmol), Pd(dppf)Cl_2 (15 mg, 0.02 mmol), and K_2CO_3 (83 mg, 0.6 mmol). The resulting reaction mixture was stirred at 90 °C under nitrogen atmosphere for 12 h. The reaction mixture was diluted with water and extracted with EtOAc (3 × 10 mL). The combined organic layer was dried over Na_2SO_4 and concentrated under reduced pressure, and the crude material was purified by flash chromatography (10% MeOH/CH_2Cl_2) to obtain compound **31l** as a white solid (40 mg, 71.6%). R_f = 0.58 (10% MeOH/CH_2Cl_2). ^{1}H NMR (500 MHz, $CDCl_3$) δ 7.88−7.81 (m, 2H), 7.45 (dd, J = 10.6, 4.8 Hz, 2H), 7.37−7.27 (m, 1H), 7.24 (dd, J = 7.5, 1.1 Hz, 1H), 7.14 (t, J = 7.7 Hz, 1H), 7.08 (dd, J = 7.9, 1.1 Hz, 1H), 5.23 (bs, 2H), 3.91 (t, J = 7.3 Hz, 2H), 1.94−1.67 (m, 2H), 1.54−1.25 (m, 4H), 0.91 (t, J = 7.1 Hz, 3H). ^{13}C NMR (126 MHz, $CDCl_3$) δ 153.61, 139.31, 139.06, 134.69, 129.52, 129.26, 128.40, 126.97, 121.49, 120.15, 107.03, 43.02, 29.25, 28.84, 22.54, 14.08. MS (ESI-TOF) for $C_{18}H_{21}N_3$ $[M + H]^+$ calculated 280.1808, found 280.1877.

*4-Benzyl-1-pentyl-1H-benzo[d]imidazol-2-amine (**31m**).* To a solution of compound **31i** (56 mg, 0.2 mmol) in THF (1 mL) were added benzylzinc bromide (1.2 mL, 0.6 mmol, 0.5 M in THF) and Pd(dppf)Cl_2 (15 mg, 0.02 mmol). The resulting reaction mixture was stirred at 70 °C under nitrogen atmosphere for 12 h. The reaction mixture was diluted with water and extracted with EtOAc (3 × 10 mL). The combined organic layer was dried over Na_2SO_4 and concentrated under reduced pressure. The crude material was purified by flash chromatography (10% MeOH/CH_2Cl_2) to obtain the compound **31m** as a white solid (44 mg, 75%). R_f = 0.60 (10% MeOH/CH_2Cl_2). ^{1}H NMR (500 MHz, $CDCl_3$) δ 7.32−7.27 (m, 3H), 7.25 (s, 1H), 7.20−7.15 (m, 1H), 7.05 (t, J = 7.7 Hz, 1H), 6.99 (d, J = 7.1 Hz, 1H), 6.90 (d, J = 7.3 Hz, 1H), 4.25 (s, 2H), 3.95 (t, J = 7.3 Hz, 2H), 1.82−1.72 (m, 2H), 1.42−1.33 (m, 4H), 0.89 (t, J = 7.0 Hz, 3H). ^{13}C NMR (126 MHz, $CDCl_3$) δ 152.10, 140.22, 136.03, 132.59, 129.11, 128.42, 128.01, 126.03, 122.83, 121.09, 106.46, 43.12, 36.62, 28.98, 28.46, 22.37, 13.91. MS (ESI-TOF) for $C_{19}H_{23}N_3$ $[M + H]^+$ calculated 294.1965, found 294.2039.

*1-Benzyloxy-3-fluoro-2-nitro-benzene (**32**).* To a solution of compound **28f** (318 mg, 2 mmol) in DMF (10 mL) were added K_2CO_3 (552 mg, 4 mmol) and benzyl alcohol (226 μL, 2.2 mmol). The reaction mixture was stirred for 12 h at 60 °C. The reaction mixture was cooled to room temperature, diluted with water, and extracted with EtOAc (3 × 30 mL). The combined organic layer was dried over Na_2SO_4 and concentrated under reduced pressure, and the crude material was purified by silica gel column chromatography (10% EtOAc/hexanes) to obtain the compound **32** as yellow oil (400 mg, 81%). R_f = 0.2 (10% EtOAc/hexanes). ^{1}H NMR (500 MHz, $CDCl_3$) δ 7.43−7.29 (m, 6H), 6.89−6.78 (m, 2H), 5.20 (s, 2H). ^{13}C NMR (126 MHz, $CDCl_3$) δ 154.69 (d, J = 257.0 Hz), 151.69 (d, J = 2.4 Hz), 135.16, 131.90 (d, J = 9.7 Hz), 128.93, 128.61, 127.19, 109.74 (d, J = 3.3 Hz), 109.02, 108.87, 71.59.

Compound **33** was synthesized similarly as compound **25a**.

*(3-Benzyloxy-2-nitro-phenyl)-pentyl-amine (**33**).* Compound **32** was used as reagent. Red oil (238 mg, 76%). R_f = 0.5 (10% EtOAc/hexanes). ^{1}H NMR (500 MHz, $CDCl_3$) δ 7.45 (dd, J = 8.0, 1.0 Hz, 2H), 7.41−7.35 (m, 2H), 7.31 (ddd, J = 7.3, 3.8, 1.3 Hz, 1H), 7.20 (t, J = 8.4 Hz, 1H), 6.40−6.34 (m, 1H), 6.29 (dd, J = 8.2, 0.9 Hz, 1H), 6.16 (bs, 1H), 5.15 (s, 2H), 3.17 (td, J = 7.1, 5.2 Hz, 2H), 1.71−1.61 (m, 2H), 1.43−1.32 (m, 4H), 0.92 (t, J = 7.1 Hz, 3H). ^{13}C NMR (126 MHz, $CDCl_3$) δ 154.28, 144.55, 136.27, 133.62, 128.72, 128.10, 127.64, 127.06, 105.48, 100.89, 71.06, 43.61, 29.31, 28.90, 22.54, 14.12. MS (ESI-TOF) for $C_{18}H_{22}N_2O_3$ $[M + H]^+$ calculated 315.1703, found 315.1664.

Compound **35** was synthesized similarly as compound **18**.

*4-Benzyloxy-1-pentyl-1H-benzoimidazol-2-ylamine (**35**).* Compound **33** was used as reagent. White solid (49 mg, 79%). R_f = 0.5 (10% MeOH/CH_2Cl_2). ^{1}H NMR (500 MHz, $CDCl_3$) δ 7.51 (dd, J = 7.9, 0.9 Hz, 2H), 7.39−7.34 (m, 2H), 7.32−7.27 (m, 1H), 6.94 (t, J = 8.0 Hz, 1H), 6.75 (dd, J = 8.0, 0.7 Hz, 1H), 6.66 (dd, J = 8.0, 0.5 Hz, 1H), 5.28 (s, 2H), 4.80 (bs, 2H), 3.85 (t, J = 7.2 Hz, 2H), 1.80−1.70 (m, 2H), 1.39−1.29 (m, 4H), 0.89 (t, J = 7.0 Hz, 3H). ^{13}C NMR (126 MHz, $CDCl_3$) δ 152.41, 148.68, 137.82, 135.87, 131.56, 128.54, 127.79, 127.78, 120.25, 105.07, 101.73, 70.66, 43.16, 29.19, 28.92, 22.53, 14.07. MS (ESI-TOF) for $C_{19}H_{23}N_3O$ $[M + H]^+$ calculated 310.1914, found 310.1954.

dx.doi.org/10.1021/jm500701q | J. Med. Chem. 2014, 57, 7325−7341

*2-Amino-1-pentyl-1H-benzoimidazol-4-ol (**36**).* To a solution of compound **35** (31 mg, 0.1 mmol) in anhydrous MeOH (5 mL) was added a catalytic amount of 10% Pd on carbon. The reaction mixture was subjected to hydrogenolysis at 30 psi H_2 pressure for 3 h. The reaction mixture was filtered, and the filtrate was concentrated under the reduced pressure. The crude material was purified by silica gel column chromatography (20% MeOH/CH_2Cl_2) to obtain the compound **36** as a off-white solid (17 mg, 78%). R_f = 0.4 (20% MeOH/CH_2Cl_2). ^{1}H NMR (500 MHz, DMSO) δ 9.35 (bs, 1H), 6.72 (t, J = 7.8 Hz, 1H), 6.64 (d, J = 7.3 Hz, 1H), 6.48−6.31 (m, 3H), 3.92 (t, J = 7.2 Hz, 2H), 1.66−1.57 (m, 2H), 1.35−1.20 (m, 4H), 0.84 (t, J = 7.0 Hz, 3H). ^{13}C NMR (126 MHz, $CDCl_3$) δ 151.81, 146.78, 134.74, 127.54, 121.91, 109.14, 99.78, 43.21, 29.15, 28.65, 22.50, 14.03. MS (ESI-TOF) for $C_{12}H_{17}N_3O$ $[M + H]^+$ calculated 220.1444, found 220.1470.

*3-Nitro-N1-pentyl-benzene-1,2-diamine (**38**).* To a solution of compound **37** (153 mg, 1 mmol) in DMF (5 mL) were added K_2CO_3 (276 mg, 2 mmol) and 1-iodopentane (143 μL, 1.1 mmol). The reaction mixture was stirred for 12 h at 50 °C. The reaction mixture was cooled to room temperature, diluted with water, and extracted with EtOAc (3 × 10 mL). The combined organic layer was dried over Na_2SO_4 and concentrated under reduced pressure, and the crude material was purified by silica gel column chromatography (5% EtOAc/hexanes) to obtain the compound **38** as a red solid (120 mg, 54%). R_f = 0.5 (10% EtOAc/hexanes). ^{1}H NMR (400 MHz, $CDCl_3$) δ 7.67 (dd, J = 8.7, 1.1 Hz, 1H), 6.85 (dd, J = 7.6, 0.9 Hz, 1H), 6.73−6.64 (m, 1H), 5.93 (bs, 2H), 3.11−3.08 (m, 3H), 1.76−1.62 (m, 2H), 1.47−1.33 (m, 4H), 0.94 (t, J = 7.0 Hz, 3H). ^{13}C NMR (126 MHz, $CDCl_3$) δ 138.52, 136.46, 133.42, 117.24, 117.22, 116.17, 45.09, 29.53, 29.38, 22.66, 14.18. MS (ESI-TOF) for $C_{11}H_{17}N_3O_2$ $[M + H]^+$ calculated 224.1394, found 224.1423.

*4-Nitro-1-pentyl-1H-benzoimidazol-2-ylamine (**39**).* To a solution of compound **38** (45 mg, 0.2 mmol) in 1:1 mixture of MeOH (1 mL) and water (1 mL) was added CNBr (63 mg, 0.6 mmol). The reaction mixture was stirred for 3 h at 60 °C. The reaction mixture was cooled to room temperature, the MeOH was removed under reduced pressure, and the remaining mixture was basified with 1.0 M aq. NaOH (to pH = 8.0) and extracted with EtOAc (3 × 20 mL). The combined organic layer was dried over Na_2SO_4 and concentrated under reduced pressure, and the crude material was purified by silica gel column chromatography (30% EtOAc/CH_2Cl_2) to obtain the compound **39** as a yellow solid (40 mg, 81%). R_f = 0.5 (10% MeOH/CH_2Cl_2). ^{1}H NMR (500 MHz, DMSO) δ 7.76 (d, J = 8.4 Hz, 1H), 7.51 (d, J = 7.7 Hz, 1H), 7.34 (bs, 2H), 6.98 (t, J = 8.0 Hz, 1H), 4.04 (t, J = 7.2 Hz, 2H), 1.69−1.56 (m, 2H), 1.35−1.19 (m, 4H), 0.84 (t, J = 7.0 Hz, 3H). ^{13}C NMR (126 MHz, DMSO) δ 158.47, 138.87, 137.88, 134.03, 116.81, 116.64, 112.99, 41.69, 28.16, 27.96, 21.92, 13.92. MS (ESI-TOF) for $C_{12}H_{16}N_4O_2$ $[M + H]^+$ calculated 249.1346, found 249.1377.

*1-Pentyl-1H-benzoimidazole-2,4-diamine (**40**).* To a solution of compound **39** (25 mg, 0.1 mmol) in anhydrous EtOAc (10 mL) was added a catalytic amount of Pt/C, and the reaction mixture was subjected to hydrogenation at 30 psi for 3 h. The reaction mixture was filtered, and the filtrate concentrated under reduced pressure. The crude material was purified using silica gel column chromatography (20% MeOH/CH_2Cl_2) to obtain **40** as off-white solid (16 mg, 74%). R_f = 0.3 (20% MeOH/CH_2Cl_2). ^{1}H NMR (400 MHz, $CDCl_3$) δ 6.90 (t, J = 7.9 Hz, 1H), 6.57 (dd, J = 8.0, 0.8 Hz, 1H), 6.48 (dd, J = 7.7, 0.9 Hz, 1H), 4.52 (bs, 2H), 3.86 (t, J = 7.3 Hz, 2H), 3.69 (bs, 2H), 1.81−1.73 (m, 2H), 1.40−1.30 (m, 4H), 0.89 (t, J = 7.0 Hz, 3H). ^{13}C NMR (126 MHz, $CDCl_3$) δ 151.38, 136.16, 134.62, 129.31, 121.20, 107.17, 99.06, 43.22, 29.20, 28.88, 22.51, 14.06. MS (ESI-TOF) for $C_{12}H_{18}N_4$ $[M + H]^+$ calculated 219.1604, found 219.1630.

Molecular Modeling and Induced Fit Docking. Quantum mechanics/molecular mechanics (QM/MM) methods[74,75] were used as reported earlier[32] for induced fit docking. Correct bond orders were assigned, hydrogen atoms were added to the residues, and formal partial charges were assigned to atoms using OPLS-all atom force field.[76] The docking grid was generated using co-crystallized ligand as grid center. Ligands were modeled in Schrödinger molecular modeling software (Schrödinger, New York, NY) and were minimized to a gradient of 0.001KCal/MolÅ^2. The QM charges for ligands were obtained from Jaguar (Schrödinger), using the 3-21G basis set with the BLYP density functional theory.[77] Initial docking was performed with Glide[78] using 0.5 van der Waals (vdW) radius scaling factor for both ligand and protein. This soft docking procedure was applied to generate diverse docking solutions, and top 20 poses for each ligand were retained. Finally, each ligand was redocked into its corresponding structures, and the resulting complexes were ranked according to GlideScore.[79]

Human TLR-2/-3/-4/-5/-7/-8/-9 and NOD-1/-2 Reporter Gene Assays (NF-κB Induction). The induction of NF-κB was quantified using human TLR-2/3/-4/-5/-7/-8/-9- and NOD-1/NOD-2-specific, rapid-throughput, liquid handler-assisted reporter gene assays as previously described by us.[31,33,37,39,43] HEK293 cells stably co-transfected with the appropriate hTLR (or NOD) and secreted alkaline phosphatase (sAP) were maintained in HEK-Blue Selection medium. Stable expression of secreted alkaline phosphatase (sAP) under control of NF-κB/AP-1 promoters is inducible by appropriate TLR/NOD agonists, and extracellular sAP in the supernatant is proportional to NF-κB induction. Reporter cells were incubated at a density of ~10^5 cells/ml in a volume of 80 μL/well, in 384-well, flat-bottomed, cell culture-treated microtiter plates in the presence of graded concentrations of stimuli. sAP was assayed spectrophotometrically using an alkaline phosphatase-specific chromogen (present in HEK-detection medium as supplied by the vendor) at 620 nm. Antagonistic activities were examined by incubating human NOD-1/-2 reporter cells with graded concentrations of test compounds in the presence of 100 ng/mL of C_{12}-iE-DAP[39] or 10 μg/mL murabutide[45] (NOD-2).

Immunoassays for Cytokines. Fresh human peripheral blood mononuclear cells (hPBMC) were isolated from human blood obtained by venipuncture with informed consent and as per institutional guidelines on Ficoll-Hypaque gradients as described elsewhere.[28] Aliquots of PBMCs (10^5 cells in 100 μL/well) were stimulated for 12 h with graded concentrations of test compounds. Supernatants were isolated by centrifugation and were assayed in duplicates using analyte-specific multiplexed cytokine/chemokine bead array assays as reported by us previously.[28]

Flow-Cytometric Immunostimulation Experiments. CD69 upregulation was determined by flow cytometry using protocols published by us previously.[28,32] Briefly, heparin-anticoagulated whole blood samples were obtained by venipuncture from healthy human volunteers with informed consent and as per guidelines approved by the University of Kansas Human Subjects Experimentation Committee. Aliquots of whole human blood samples were stimulated with graded concentrations of **31a**, reference compound(s), or medium (negative control) in 96-well polypropylene plates and incubated at 37 °C overnight. Following incubation, 200 μL aliquots of anticoagulated whole blood were stained with 20 μL of fluorochrome-conjugated antibodies at 37 °C in the dark for 30 min. For triple color flow cytometry experiments, CD3-PE, CD56-APC, and CD69-PE-Cy7 were used to analyze CD69 activation of each of the main peripheral blood lymphocyte populations: natural killer lymphocytes (NK cells: $CD3^-CD56^+$), cytokine-induced killer phenotype (CIK cells: $CD3^+CD56^+$), nominal B lymphocytes ($CD3^-CD56^-$), and nominal T lymphocytes ($CD3^+CD56^-$). Following staining, erythrocytes were lysed and leukocytes fixed in one step using Whole Blood Lyse/Fix Buffer (Becton-Dickinson Biosciences, San Jose, CA). Flow cytometry was performed using a BD FACSArray instrument on 100,000 gated events. Postacquisition analyses were performed using FlowJo v 7.0 software (Treestar, Ashland, OR).

■ ASSOCIATED CONTENT

Supporting Information

Characterization data (^{1}H, ^{13}C, mass spectra) and LC-MS analyses of key precursors and final compounds. This material is available free of charge via the Internet at http://pubs.acs.org.

■ AUTHOR INFORMATION

Corresponding Author

*E-mail: sdavid@ku.edu. Tel: 785-864-1610. Fax: 785-864-1961.

Notes

The authors declare no competing financial interest.

■ ACKNOWLEDGMENTS

This work was supported by NIH/NIAID contract HSN272200900033C. Support for NMR instrumentation was provided by NIH Shared Instrumentation grant no. S10RR024664 and NSF Major Research Instrumentation grant no. 0320648.

■ ABBREVIATIONS USED:

CCR1, C-C chemokine receptor type 1; DIPEA, *N*,*N*-Diisopropylethylamine; EC_{50}, Half-maximal effective concentration; ESI-TOF, Electrospray ionization-time-of-flight; HEK, Human embryonic kidney; HIV, Human immunodeficiency virus; HOBt, 1-Hydroxybenzotriazole; IFN, Interferon; IL, Interleukin; IRAK-4, Interleukin-1 receptor-associated kinase 4; LRR, Leucine-rich repeat; LPS, Lipopolysaccharide; MHC, Major histocompatibility complex; MPL, monophosphoryl lipid A; NF-κB, Nuclear factor-κB; NK, Natural killer; NLR, Nod-like receptor; NOD-1 and -2, Nucleotide-binding oligomerization domain-containing protein 1 and 2; PBMCs, Peripheral blood mononuclear cells; sAP, Secreted alkaline phosphatase; T_H1, Helper T lymphocyte, type 1; T_H2, Helper T lymphocyte, type 2; TIR, Toll/Interleukin-1 receptor; TLR, Toll-like receptor; WHO, World Health Organization; TNF-α, Tumor necrosis factor-α

■ REFERENCES

(1) Plotkin, S. A. Vaccines in the 21st century. *Infect. Dis. Clin. North Am.* **2001**, *15*, 307−327.
(2) Plotkin, S. A. Vaccines: the fourth century. *Clin. Vacc. Immunol. CVI* **2009**, *16*, 1709−1719.
(3) World Health Organization. *Antimicrobial resistance: global report on surveillance 2014*; WHO: Geneva, Switzerland, 2014; http://www.who.int/drugresistance/documents/surveillancereport/en/.
(4) Thomas-Crusells, J.; McElhaney, J. E.; Aguado, M. T. Report of the *ad-hoc* consultation on aging and immunization for a future WHO research agenda on life-course immunization. *Vaccine* **2012**, *30*, 6007−6012.
(5) Poland, G. A.; Belmin, J.; Langley, J.; Michel, J. P.; Van Damme, P.; Wicker, S. A global prescription for adult immunization: time is catching up with us. *Vaccine* **2010**, *28*, 7137−7139.
(6) Poland, G. A.; Jacobson, R. M.; Ovsyannikova, I. G. Trends affecting the future of vaccine development and delivery: the role of demographics, regulatory science, the anti-vaccine movement, and vaccinomics. *Vaccine* **2009**, *27*, 3240−3244.
(7) Falsey, A. R.; Treanor, J. J.; Tornieporth, N.; Capellan, J.; Gorse, G. J. Randomized, double-blind controlled phase 3 trial comparing the immunogenicity of high-dose and standard-dose influenza vaccine in adults 65 years of age and older. *J. Infect. Dis.* **2009**, *200*, 172−180.
(8) Banzhoff, A.; Gasparini, R.; Laghi-Pasini, F.; Staniscia, T.; Durando, P.; Montomoli, E.; Capecchi, P. L.; di Giovanni, P.; Sticchi, L.; Gentile, C.; Hilbert, A.; Brauer, V.; Tilman, S.; Podda, A. MF59-adjuvanted H5N1 vaccine induces immunologic memory and heterotypic antibody responses in non-elderly and elderly adults. *PLoS One* **2009**, *4*, e4384.
(9) Ansaldi, F.; Bacilieri, S.; Durando, P.; Sticchi, L.; Valle, L.; Montomoli, E.; Icardi, G.; Gasparini, R.; Crovari, P. Cross-protection by MF59-adjuvanted influenza vaccine: neutralizing and haemagglutination-inhibiting antibody activity against A(H3N2) drifted influenza viruses. *Vaccine* **2008**, *26*, 1525−1529.
(10) Tagliabue, A.; Rappuoli, R. Vaccine adjuvants: the dream becomes real. *Hum. Vaccines* **2008**, *4*, 347−349.
(11) Schmidt, C. S.; Morrow, W. J.; Sheikh, N. A. Smart adjuvants. *Expert Rev.Vaccines* **2007**, *6*, 391−400.
(12) Kwissa, M.; Kasturi, S. P.; Pulendran, B. The science of adjuvants. *Expert Rev. Vaccines* **2007**, *6*, 673−684.
(13) Chiarella, P.; Massi, E.; De Robertis, M.; Signori, E.; Fazio, V. M. Adjuvants in vaccines and for immunisation: current trends. *Expert Opin. Biol. Ther.* **2007**, *7*, 1551−1562.
(14) Aguilar, J. C.; Rodriguez, E. G. Vaccine adjuvants revisited. *Vaccine* **2007**, *25*, 3752−3762.
(15) Brito, L. A.; Malyala, P.; O'Hagan, D. T. Vaccine adjuvant formulations: a pharmaceutical perspective. *Semin. Immunol.* **2013**, *25*, 130−145.
(16) Garcon, N.; Segal, L.; Tavares, F.; Van Mechelen, M. The safety evaluation of adjuvants during vaccine development: the AS04 experience. *Vaccine* **2011**, *29*, 4453−4459.
(17) Esposito, S.; Birlutiu, V.; Jarcuska, P.; Perino, A.; Man, S. C.; Vladareanu, R.; Meric, D.; Dobbelaere, K.; Thomas, F.; Descamps, D. Immunogenicity and safety of human papillomavirus-16/18 AS04-adjuvanted vaccine administered according to an alternative dosing schedule compared with the standard dosing schedule in healthy women aged 15 to 25 years: results from a randomized study. *Pediatr. Infect. Dis. J.* **2011**, *30*, e49−e55.
(18) Glenny, A. T.; Pope, C. G.; Waddington, H.; Wallace, V. The antigenic value of toxoid precipitated by potassium-alum. *J. Pathol. Bacteriol.* **1926**, *29*, 38−45.
(19) Relyveld, E. H.; Bizzini, B.; Gupta, R. K. Rational approaches to reduce adverse reactions in man to vaccines containing tetanus and diphtheria toxoids. *Vaccine* **1998**, *16*, 1016−1023.
(20) Gupta, R. K. Aluminum compounds as vaccine adjuvants. *Adv. Drug Delivery Rev.* **1998**, *32*, 155−172.
(21) Hoffmann, J.; Akira, S. Innate immunity. *Curr. Opin. Immunol.* **2013**, *25*, 1−3.
(22) Kumagai, Y.; Akira, S. Identification and functions of pattern-recognition receptors. *J. Allergy Clin. Immunol.* **2010**, *125*, 985−992.
(23) Kawai, T.; Akira, S. The role of pattern-recognition receptors in innate immunity: update on Toll-like receptors. *Nat. Immunol.* **2010**, *11*, 373−384.
(24) Loo, Y. M.; Gale, M., Jr. Immune signaling by RIG-I-like receptors. *Immunity* **2011**, *34*, 680−692.
(25) Kersse, K.; Bertrand, M. J.; Lamkanfi, M.; Vandenabeele, P. NOD-like receptors and the innate immune system: coping with danger, damage and death. *Cytokine Growth Factor Rev.* **2011**, *22*, 257−276.
(26) Clarke, T. B.; Weiser, J. N. Intracellular sensors of extracellular bacteria. *Immunol. Rev.* **2011**, *243*, 9−25.
(27) Cottalorda, A.; Verschelde, C.; Marcais, A.; Tomkowiak, M.; Musette, P.; Uematsu, S.; Akira, S.; Marvel, J.; Bonnefoy-Berard, N. TLR2 engagement on CD8 T cells lowers the threshold for optimal antigen-induced T cell activation. *Eur. J. Immunol.* **2006**, *36*, 1684−1693.
(28) Kokatla, H. P.; Sil, D.; Tanji, H.; Ohto, U.; Malladi, S. S.; Fox, L. M.; Shimizu, T.; David, S. A. Structure-based design of novel human Toll-like receptor 8 agonists. *ChemMedChem* **2014**, *9*, 719−723.
(29) Yoo, E.; Crall, B. M.; Balakrishna, R.; Malladi, S. S.; Fox, L. M.; Hermanson, A. R.; David, S. A. Structure-activity relationships in Toll-like receptor 7 agonistic 1*H*-imidazo[4, 5-*c*]pyridines. *Org. Biomol. Chem.* **2013**, *11*, 6526−6545.
(30) Salunke, D. B.; Connelly, S. W.; Shukla, N. M.; Hermanson, A. R.; Fox, L. M.; David, S. A. Design and development of stable, water-soluble, human Toll-like receptor 2 specific monoacyl lipopeptides as candidate vaccine adjuvants. *J. Med. Chem.* **2013**, *56*, 5885−5900.
(31) Kokatla, H. P.; Yoo, E.; Salunke, D. B.; Sil, D.; Ng, C. F.; Balakrishna, R.; Malladi, S. S.; Fox, L. M.; David, S. A. Toll-like receptor-8 agonistic activities in C2, C4, and C8 modified thiazolo[4, 5-*c*]quinolines. *Org. Biomol. Chem.* **2013**, *11*, 1179−1198.
(32) Kokatla, H. P.; Sil, D.; Malladi, S. S.; Balakrishna, R.; Hermanson, A. R.; Fox, L. M.; Wang, X.; Dixit, A.; David, S. A. Exquisite selectivity for human Toll-like receptor 8 in substituted furo[2, 3-*c*]quinolines. *J. Med. Chem.* **2013**, *56*, 6871−6885.
(33) Ukani, R.; Lewis, T. C.; Day, T. P.; Wu, W.; Malladi, S. S.; Warshakoon, H. J.; David, S. A. Potent adjuvantic activity of a CCR1-agonistic bis-quinoline. *Bioorg. Med. Chem. Lett.* **2012**, *22*, 293−295.

(34) Shukla, N. M.; Salunke, D. B.; Balakrishna, R.; Mutz, C. A.; Malladi, S. S.; David, S. A. Potent adjuvanticity of a pure TLR7-agonistic imidazoquinoline dendrimer. *PLoS One* **2012**, *7*, e43612.
(35) Shukla, N. M.; Mutz, C. A.; Malladi, S. S.; Warshakoon, H. J.; Balakrishna, R.; David, S. A. Toll-Like Receptor (TLR)-7 and −8 modulatory activities of dimeric imidazoquinolines. *J. Med. Chem.* **2012**, *55*, 1106−1116.
(36) Salunke, D. B.; Yoo, E.; Shukla, N. M.; Balakrishna, R.; Malladi, S. S.; Serafin, K. J.; Day, V. W.; Wang, X.; David, S. A. Structure-activity relationships in human Toll-like receptor 8-active 2,3-diamino-furo[2,3-*c*]pyridines. *J. Med. Chem.* **2012**, *55*, 8137−8151.
(37) Salunke, D. B.; Shukla, N. M.; Yoo, E.; Crall, B. M.; Balakrishna, R.; Malladi, S. S.; David, S. A. Structure-activity relationships in human Toll-like receptor 2-specific monoacyl lipopeptides. *J. Med. Chem.* **2012**, *55*, 3353−3363.
(38) Shukla, N. M.; Lewis, T. C.; Day, T. P.; Mutz, C. A.; Ukani, R.; Hamilton, C. D.; Balakrishna, R.; David, S. A. Toward self-adjuvanting subunit vaccines: model peptide and protein antigens incorporating covalently bound Toll-like receptor-7 agonistic imidazoquinolines. *Bioorg. Med. Chem. Lett.* **2011**, *21*, 3232−3236.
(39) Agnihotri, G.; Ukani, R.; Malladi, S. S.; Warshakoon, H. J.; Balakrishna, R.; Wang, X.; David, S. A. Structure-activity relationships in nucleotide oligomerization domain 1 (Nod1) agonistic gamma-glutamyldiaminopimelic acid derivatives. *J. Med. Chem.* **2011**, *54*, 1490−1510.
(40) Agnihotri, G.; Crall, B. M.; Lewis, T. C.; Day, T. P.; Balakrishna, R.; Warshakoon, H. J.; Malladi, S. S.; David, S. A. Structure-activity relationships in Toll-like receptor 2-agonists leading to simplified monoacyl lipopeptides. *J. Med. Chem.* **2011**, *54*, 8148−8160.
(41) Wu, W.; Li, R.; Malladi, S. S.; Warshakoon, H. J.; Kimbrell, M. R.; Amolins, M. W.; Ukani, R.; Datta, A.; David, S. A. Structure-activity relationships in Toll-like receptor-2 agonistic diacylthioglycerol lipopeptides. *J. Med. Chem.* **2010**, *53*, 3198−3213.
(42) Shukla, N. M.; Mutz, C. A.; Ukani, R.; Warshakoon, H. J.; Moore, D. S.; David, S. A. Syntheses of fluorescent imidazoquinoline conjugates as probes of Toll-like receptor 7. *Bioorg. Med. Chem. Lett.* **2010**, *20*, 6384−6386.
(43) Shukla, N. M.; Malladi, S. S.; Mutz, C. A.; Balakrishna, R.; David, S. A. Structure-activity relationships in human toll-like receptor 7-active imidazoquinoline analogues. *J. Med. Chem.* **2010**, *53*, 4450−4465.
(44) Hood, J. D.; Warshakoon, H. J.; Kimbrell, M. R.; Shukla, N. M.; Malladi, S.; Wang, X.; David, S. A. Immunoprofiling toll-like receptor ligands: Comparison of immunostimulatory and proinflammatory profiles in ex vivo human blood models. *Hum. Vaccines* **2010**, *6*, 1−14.
(45) Warshakoon, H. J.; Hood, J. D.; Kimbrell, M. R.; Malladi, S.; Wu, W. Y.; Shukla, N. M.; Agnihotri, G.; Sil, D.; David, S. A. Potential adjuvantic properties of innate immune stimuli. *Hum. Vaccines* **2009**, *5*, 381−394.
(46) Shukla, N. M.; Malladi, S. S.; Day, V.; David, S. A. Preliminary evaluation of a 3*H* imidazoquinoline library as dual TLR7/TLR8 antagonists. *Bioorg. Med. Chem.* **2011**, *19*, 3801−3811.
(47) Jurk, M.; Heil, F.; Vollmer, J.; Schetter, C.; Krieg, A. M.; Wagner, H.; Lipford, G.; Bauer, S. Human TLR7 or TLR8 independently confer responsiveness to the antiviral compound R-848. *Nat. Immunol.* **2002**, *3*, 499.
(48) Gerster, J. F.; Lindstrom, K. J.; Miller, R. L.; Tomai, M. A.; Birmachu, W.; Bomersine, S. N.; Gibson, S. J.; Imbertson, L. M.; Jacobson, J. R.; Knafla, R. T.; Maye, P. V.; Nikolaides, N.; Oneyemi, F. Y.; Parkhurst, G. J.; Pecore, S. E.; Reiter, M. J.; Scribner, L. S.; Testerman, T. L.; Thompson, N. J.; Wagner, T. L.; Weeks, C. E.; Andre, J. D.; Lagain, D.; Bastard, Y.; Lupu, M. Synthesis and structure-activity-relationships of 1*H*-imidazo[4, 5-*c*]quinolines that induce interferon production. *J. Med. Chem.* **2005**, *48*, 3481−3491.
(49) Gerster, J. F.; Lindstrom, K. J.; Marszalek, G. J.; Merrill, B. A.; Mickelson, J. W.; Rice, M. J. Oxazolo, thiazolo and selenazolo [4,5-*c*]-quinolin-4-amines and analogs thereof. WO 2000006577 A1, February 10, 2000.
(50) Prince, R. B.; Rice, M. J.; Wurst, J. R.; Merrill, B. A.; Kshirsagar, T. A.; Heppner, P. D. Aryloxy and arylalkyleneoxy substituted thiazoloquinolines and thiazolonapthyridines. WO 2006009826 A1, January 26, 2006.
(51) Prince, R. B.; Merrill, B. A.; Heppner, P. D.; Kshirsagar, T. A.; Wurst, J. R.; Manske, K. J.; Rice, M. J. Alkyloxy substituted thiazoloquinolines and thioloonaphthyridines. WO 2006086449 A3, February 8, 2006.
(52) Lu, H.; Dietsch, G. N.; Matthews, M. A.; Yang, Y.; Ghanekar, S.; Inokuma, M.; Suni, M.; Maino, V. C.; Henderson, K. E.; Howbert, J. J.; Disis, M. L.; Hershberg, R. M. VTX-2337 is a novel TLR8 agonist that activates NK cells and augments ADCC. *Clin. Cancer Res.* **2012**, *18*, 499−509.
(53) Philbin, V. J.; Dowling, D. J.; Gallington, L. C.; Cortes, G.; Tan, Z.; Suter, E. E.; Chi, K. W.; Shuckett, A.; Stoler-Barak, L.; Tomai, M.; Miller, R. L.; Mansfield, K.; Levy, O. Imidazoquinoline Toll-like receptor 8 agonists activate human newborn monocytes and dendritic cells through adenosine-refractory and caspase-1-dependent pathways. *J. Allergy Clin. Immunol.* **2012**, *130*, 195−204.
(54) Levy, O.; Suter, E. E.; Miller, R. L.; Wessels, M. R. Unique efficacy of Toll-like receptor 8 agonists in activating human neonatal antigen-presenting cells. *Blood* **2006**, *108*, 1284−1290.
(55) van den Berg, J. P.; Westerbeek, E. A.; van der Klis, F. R.; Berbers, G. A.; van Elburg, R. M. Transplacental transport of IgG antibodies to preterm infants: a review of the literature. *Early Hum. Dev.* **2011**, *87*, 67−72.
(56) PrabhuDas, M.; Adkins, B.; Gans, H.; King, C.; Levy, O.; Ramilo, O.; Siegrist, C. A. Challenges in infant immunity: implications for responses to infection and vaccines. *Nat. Immunol.* **2011**, *12*, 189−194.
(57) Wood, N.; Siegrist, C. A. Neonatal immunization: where do we stand? *Curr. Opin. Infect. Dis.* **2011**, *24*, 190−195.
(58) Corbett, N. P.; Blimkie, D.; Ho, K. C.; Cai, B.; Sutherland, D. P.; Kallos, A.; Crabtree, J.; Rein-Weston, A.; Lavoie, P. M.; Turvey, S. E.; Hawkins, N. R.; Self, S. G.; Wilson, C. B.; Hajjar, A. M.; Fortuno, E. S., III; Kollmann, T. R. Ontogeny of Toll-like receptor mediated cytokine responses of human blood mononuclear cells. *PLoS One* **2010**, *5*, e15041.
(59) Kollmann, T. R.; Crabtree, J.; Rein-Weston, A.; Blimkie, D.; Thommai, F.; Wang, X. Y.; Lavoie, P. M.; Furlong, J.; Fortuno, E. S., III; Hajjar, A. M.; Hawkins, N. R.; Self, S. G.; Wilson, C. B. Neonatal innate TLR-mediated responses are distinct from those of adults. *J. Immunol.* **2009**, *183*, 7150−7160.
(60) Shaw, A. C.; Panda, A.; Joshi, S. R.; Qian, F.; Allore, H. G.; Montgomery, R. R. Dysregulation of human Toll-like receptor function in aging. *Ageing Res. Rev.* **2011**, *10*, 346−353.
(61) Shaw, A. C.; Joshi, S.; Greenwood, H.; Panda, A.; Lord, J. M. Aging of the innate immune system. *Curr. Opin. immunol.* **2010**, *22*, 507−513.
(62) Panda, A.; Qian, F.; Mohanty, S.; van Duin, D.; Newman, F. K.; Zhang, L.; Chen, S.; Towle, V.; Belshe, R. B.; Fikrig, E.; Allore, H. G.; Montgomery, R. R.; Shaw, A. C. Age-associated decrease in TLR function in primary human dendritic cells predicts influenza vaccine response. *J. Immunol.* **2010**, *184*, 2518−2527.
(63) Goronzy, J. J.; Weyand, C. M. Understanding immunosenescence to improve responses to vaccines. *Nat. Immunol.* **2013**, *14*, 428−436.
(64) Grubeck-Loebenstein, B.; Della Bella, S.; Iorio, A. M.; Michel, J. P.; Pawelec, G.; Solana, R. Immunosenescence and vaccine failure in the elderly. *Aging: Clin. Exp. Res.* **2009**, *21*, 201−209.
(65) Chen, W. H.; Kozlovsky, B. F.; Effros, R. B.; Grubeck-Loebenstein, B.; Edelman, R.; Sztein, M. B. Vaccination in the elderly: an immunological perspective. *Trends Immunol.* **2009**, *30*, 351−359.
(66) Kost, A. N.; Yu, N.; Golubeva, G. A.; Popova, A. G.; Mushket, B. Synthesis and autooxidation of 2-amino-1,3-dialkylindoles. *Chem. Heterocycl. Compd.* **1979**, *16*, 917−921.
(67) Tanji, H.; Ohto, U.; Shibata, T.; Miyake, K.; Shimizu, T. Structural reorganization of the Toll-like receptor 8 dimer induced by agonistic ligands. *Science* **2013**, *339*, 1426−1429.
(68) Mackerell, A. D., Jr. Empirical force fields for biological macromolecules: overview and issues. *J. Comput. Chem.* **2004**, *25*, 1584−604.

(69) Correa, R. G.; Khan, P. M.; Askari, N.; Zhai, D.; Gerlic, M.; Brown, B.; Magnuson, G.; Spreafico, R.; Albani, S.; Sergienko, E.; Diaz, P. W.; Roth, G. P.; Reed, J. C. Discovery and characterization of 2-aminobenzimidazole derivatives as selective NOD1 inhibitors. *Chem. Biol.* **2011**, *18*, 825−832.
(70) Gonzalez-Amaro, R.; Cortes, J. R.; Sanchez-Madrid, F.; Martin, P. Is CD69 an effective brake to control inflammatory diseases? *Trends Mol. Med.* **2013**, *19*, 625−632.
(71) Sancho, D.; Gomez, M.; Sanchez-Madrid, F. CD69 is an immunoregulatory molecule induced following activation. *Trends Immunol* **2005**, *26*, 136−140.
(72) Esplugues, E.; Sancho, D.; Vega-Ramos, J.; Martinez, C.; Syrbe, U.; Hamann, A.; Engel, P.; Sanchez-Madrid, F.; Lauzurica, P. Enhanced antitumor immunity in mice deficient in CD69. *J. Exp. Med.* **2003**, *197*, 1093−1106.
(73) Sancho, D.; Gomez, M.; Viedma, F.; Esplugues, E.; Gordon-Alonso, M.; Garcia-Lopez, M. A.; de la Fuente, H.; Martinez, A. C.; Lauzurica, P.; Sanchez-Madrid, F. CD69 downregulates autoimmune reactivity through active transforming growth factor-beta production in collagen-induced arthritis. *J. Clin. Invest.* **2003**, *112*, 872−882.
(74) Alves, C. N.; Marti, S.; Castillo, R.; Andres, J.; Moliner, V.; Tunon, I.; Silla, E. A quantum mechanics/molecular mechanics study of the protein-ligand interaction for inhibitors of HIV-1 integrase. *Chemistry* **2007**, *13*, 7715−7724.
(75) Murphy, R. B.; Philipp, D. M.; Friesner, R. A. A mixed quantum mechanics/molecular mechanics (QM/MM) method for large-scale modeling of chemistry in protein environments. *J. Comput. Chem.* **2000**, *21*, 1442−1457.
(76) Jorgensen, W. L.; Schyman, P. Treatment of Halogen Bonding in the OPLS-AA Force Field; Application to Potent Anti-HIV Agents. *J. Chem. Theory Comput.* **2012**, *8*, 3895−3801.
(77) Antony, J.; Grimme, S. Density functional theory including dispersion corrections for intermolecular interactions in a large benchmark set of biologically relevant molecules. *Phys. Chem. Chem. Phys.* **2006**, *8*, 5287−5293.
(78) Repasky, M. P.; Shelley, M.; Friesner, R. A. Flexible ligand docking with Glide. *Currurent Protocols in Bioinformatics*; Wiley and Sons, Inc.: Hoboken, NJ, 2007; Chapter 8, Unit 8.12. DOI: 10.1002/0471250953.bi0812s18.
(79) Halgren, T. A.; Murphy, R. B.; Friesner, R. A.; Beard, H. S.; Frye, L. L.; Pollard, W. T.; Banks, J. L. Glide: a new approach for rapid, accurate docking and scoring. 2. Enrichment factors in database screening. *J. Med. Chem.* **2004**, *47*, 1750−1759.